© 2015. Published by The Company of Biologists Ltd | Development (2015) 142, 2894-2903 doi:10.1242/dev.120204

RESEARCH ARTICLE

STEM CELLS AND REGENERATION

# Osteoblast de- and redifferentiation are controlled by a dynamic response to retinoic acid during zebrafish fin regeneration

**Nicola Blum[1,2] and Gerrit Begemann[1,*]**

## ABSTRACT

Zebrafish restore amputated fins by forming tissue-specific blastema cells that coordinately regenerate the lost structures. Fin amputation triggers the synthesis of several diffusible signaling factors that are required for regeneration, raising the question of how cell lineage-specific programs are protected from regenerative crosstalk between neighboring fin tissues. During fin regeneration, osteoblasts revert from a non-cycling, mature state to a cycling, preosteoblastic state to establish a pool of progenitors within the blastema. After several rounds of proliferation, preosteoblasts redifferentiate to produce new bone. Blastema formation and proliferation are driven by the continued synthesis of retinoic acid (RA). Here, we find that osteoblast dedifferentiation and redifferentiation are inhibited by RA signaling, and we uncover how the bone regenerative program is achieved against a background of massive RA synthesis. Stump osteoblasts manage to contribute to the blastema by upregulating expression of the RA-degrading enzyme *cyp26b1*. Redifferentiation is controlled by a presumptive gradient of RA, in which high RA levels towards the distal tip of the blastema suppress redifferentiation. We show that this might be achieved through a mechanism involving repression of Bmp signaling and promotion of Wnt/β-catenin signaling. In turn, *cyp26b1*$^{+}$ fibroblast-derived blastema cells in the more proximal regenerate serve as a sink to reduce RA levels, thereby allowing differentiation of neighboring preosteoblasts. Our findings reveal a mechanism explaining how the osteoblast regenerative program is protected from adverse crosstalk with neighboring fibroblasts that advances our understanding of the regulation of bone repair by RA.

**KEY WORDS: Bone, Osteoblast, *Cyp26b1*, Caudal fin, Zebrafish, R115866, Osteoclast**

## INTRODUCTION

Regeneration of amphibian and fish appendages proceeds through epimorphic regeneration, in which a blastema of cycling progenitor cells forms at the wound site. The blastema harbors a mixture of cells with distinct origins and fate-restricted potential that coordinately regenerate the lost appendage (Gemberling et al., 2013; Tanaka and Reddien, 2011). The zebrafish caudal fin, which completely regrows within two weeks upon amputation, has emerged as a powerful model to study the underlying cellular and molecular mechanisms of appendage regeneration. Amputation triggers successive steps (wound healing, blastema formation and regenerative outgrowth) that finally restore the original tissues, including bone, connective tissue, blood vessels, nerves, epidermis and pigment cells (Akimenko et al., 2003; Poss et al., 2003). Several signaling pathways have been implicated in fin regeneration (e.g. FGF, Igf, RA and Wnt/β-catenin signaling) (Blum and Begemann, 2012; Chablais and Jazwinska, 2010; Poss et al., 2000; Stewart et al., 2014; Stoick-Cooper et al., 2007; Wehner et al., 2014; Whitehead et al., 2005). However, our understanding of their tissue-specific functions is very limited. Identifying the signals that act on the distinct cell lineages is therefore a crucial next step towards a thorough understanding of fin regeneration. Another major unresolved question is how regenerative programs specific for a particular cell lineage are protected from regenerative crosstalk between neighboring fin tissues. For example, high concentrations of diffusible signals required by many cells might interfere with a subset that must avoid them.

The skeletal elements of the fin, the fin rays, run from proximal to distal and are separated by soft interray tissue (Akimenko et al., 2003). Each fin ray is made up of two opposed and segmented hemirays, derived from intramembranous ossification that surround a soft core of fibroblasts, blood vessels, nerves and pigment cells (Fig. 1A). The bone matrix is laid down by osteoblasts that line up along the bone surface. During fin regeneration osteoblasts switch from a non-cycling, matrix-producing (mature) state to a cycling, less differentiated (preosteoblastic) state, and vice versa (supplementary material Fig. S1; Knopf et al., 2011; Sousa et al., 2011; Stewart and Stankunas, 2012). This remarkable behavior allows rapid replacement of lost bone. Upon amputation, mature osteoblasts next to the amputation site become proliferative and migrate towards the wound site. In the nascent blastema, preosteoblasts align at proximal lateral positions, thereby forming a spatially restricted subpopulation of the blastema. After several rounds of division, preosteoblasts redifferentiate to form new bone tissue. Differentiation progresses in a distal-to-proximal direction, so that fast cycling preosteoblasts at the distal leading edge of aligned osteoblasts become slow-cycling differentiating cells, which subsequently mature into non-cycling matrix-producing cells (Stewart et al., 2014). Despite their dedifferentiation, osteoblasts remain lineage restricted (Knopf et al., 2011; Stewart and Stankunas, 2012). To achieve proper reconstitution of lost bone, appropriate ratios between osteoblast dedifferentiation, proliferation and redifferentiation must be tightly controlled. However, the molecular mechanisms that control the transition between the distinct differentiation states within the osteoblast lineage have only recently begun to be addressed. Wnt/β-catenin and BMP signaling have been shown to regulate preosteoblast proliferation and differentiation via opposing activities (Stewart et al., 2014). The signals that control osteoblast dedifferentiation in the stump are unknown so far.

Retinoic acid (RA) has been shown to play multiple roles in bone development and repair by exerting pleiotropic effects on cells of the chondroblast, osteoblast and osteoclast lineages (Adams et al.,

[1]Developmental Biology, University of Bayreuth, Bayreuth 95440, Germany. [2]RTG1331, Department of Biology, University of Konstanz, Konstanz 78457, Germany.

*Author for correspondence (gerrit.begemann@uni-bayreuth.de)

**Received 23 November 2014; Accepted 27 July 2015**

Development (2015) 142, 2894-2903 doi:10.1242/dev.120204

2007; Allen et al., 2002; Conaway et al., 2013; Dranse et al., 2011; Koyama et al., 1999; Laue et al., 2008, 2011; Li et al., 2010; Lie and Moren, 2012; Lind et al., 2013; Nallamshetty et al., 2013; Song et al., 2005; Spoorendonk et al., 2008; Weston et al., 2003; Williams et al., 2009). Although partially conflicting results were reported, the general consensus for osteoblastogenesis is that RA signaling restricts osteoblast differentiation but promotes subsequent bone matrix synthesis by mature osteoblasts.

Fin amputation triggers massive RA synthesis that is indispensable for blastema formation and maintenance (Blum and Begemann, 2012, 2013), raising the question of how the osteoblast lineage deals with the massive background of RA signaling. Here, we demonstrate that two key steps of the osteoblast regenerative program, osteoblast dedifferentiation and subsequent redifferentiation, are adversely affected by RA from neighboring tissues. Moreover, we provide a conceptual framework for understanding how bone regeneration is achieved during fin regeneration.

## RESULTS

### Aldh1a2 and Cyp26b1 cooperate to control osteoblast activity in the uninjured fin

The zebrafish caudal fin grows throughout life. Fin growth is achieved via the sequential, distal addition of new segments to each fin ray (Haas, 1962). At the same time, hemiray thickness increases over time by adding new bone matrix along the entire fin length, meaning that hemirays are thicker in older fish and at more proximal positions (Fig. 1B; supplementary material Fig. S2A). Thus, osteoblasts in the uninjured fin continuously synthesize basal levels of matrix. In larval zebrafish, RA promotes bone matrix synthesis (Laue et al., 2008; Li et al., 2010; Spoorendonk et al., 2008). We therefore expected a comparable role for RA signaling in osteoblasts in the adult fin. We detected expression of the RA synthesizing-enzyme *aldh1a2* in proximity to hemirays (supplementary material Fig. S2B). Using *aldh1a2:gfp* fish (Pittlik and Begemann, 2012), *aldh1a2*-expressing cells could be identified as fibroblasts adjacent to osteoblasts (Fig. 1C). Osteoblasts were visualized by immunohistochemistry (IHC) for ZNS-5, an uncharacterized cell surface antigen specifically present on osteoblasts, irrespective of their differentiation status (Johnson and Weston, 1995; Knopf et al., 2011). This finding suggests that fin osteoblasts receive RA from neighboring fibroblasts. We have previously shown that intraperitoneal (IP) injection of RA efficiently enhances RA levels in the adult fin (Blum and Begemann, 2012). A single injection of RA resulted in enhanced expression of the bone matrix genes *osteocalcin* (*osc*) (also known as *bglap*), *osteonectin* (*osn*), *collagen* (*col*) *1a1a* and *col10a1* in the uninjured fin 10 h after injection (Fig. 1D). Conversely, breakdown of endogenous RA levels via overexpression of the RA-degrading enzyme *cyp26a1* in *hsp70l:cyp26a1* fish (Blum and Begemann, 2012) caused downregulation within 12 h after a single heat shock (Fig. 1D). Moreover, the hemiray surface was fully covered by osteoblasts after 10 days of RA inhibition in *hsp70l:cyp26a1* fish (supplementary material Fig. S2C), indicating that downregulation of bone matrix genes was not due to osteoblast death. Together, these data show that RA signaling positively regulates bone matrix synthesis in the adult uninjured fin.

In order to maintain the right balance between stiffness and flexibility of hemirays, matrix synthesis has to be tightly controlled. The RA-degrading enzyme Cyp26b1 attenuates osteoblast activity in larval zebrafish (Laue et al., 2008; Spoorendonk et al., 2008). *In situ* hybridization (ISH) on uninjured fins revealed expression of *cyp26b1* in fin osteoblasts (Fig. 1E). By contrast, expression of the two other

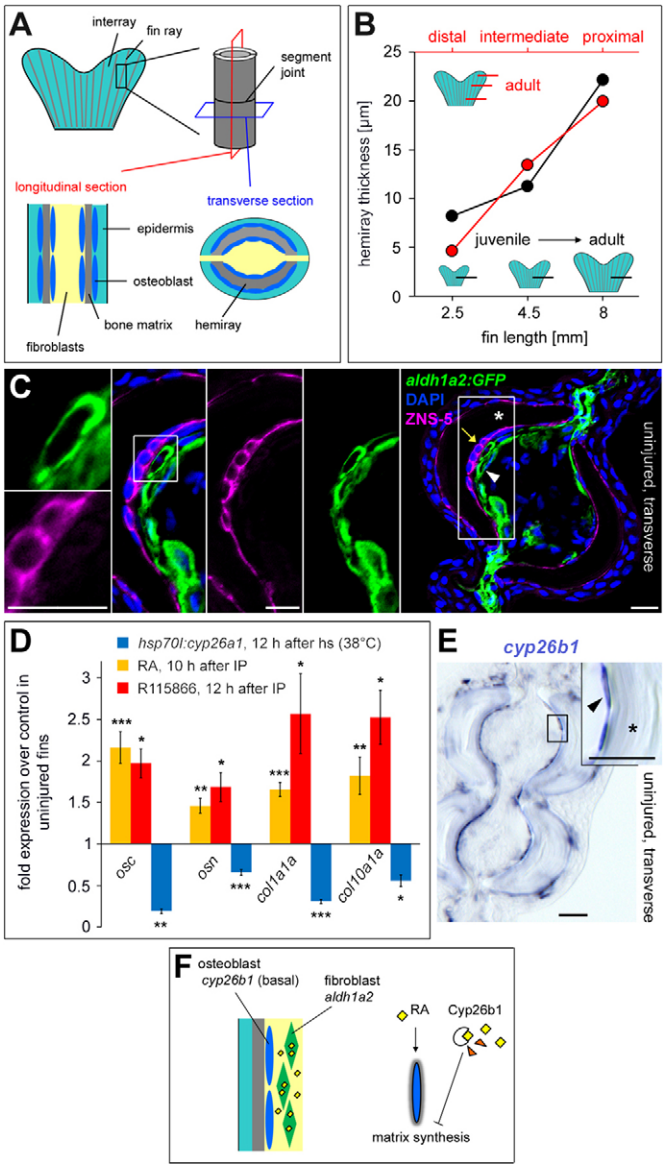


**Fig. 1. Bone matrix synthesis in the uninjured fin is controlled by RA production and degradation.** (A) Overview of relevant structures and tissue types of a fin ray. (B) Mean hemiray thickness at different positions along the proximodistal axis in adult fish (red) and at an intermediate position in fins of different lengths (black) show that hemirays are thicker in older fish (longer fin) and at more proximal positions. (C) IHC for ZNS-5 and GFP in *aldh1a2:gfp* fish in the uninjured fin reveals *aldh1a2* expression in fibroblasts (arrowhead) adjacent to osteoblasts (arrow). Asterisk indicates bone matrix. (D) RA and R115866 injections upregulate expression of bone matrix genes. Conversely, inhibition of RA signaling in *hsp70l:cyp26a1* fish downregulates expression (qPCR analysis). (E) ISH demonstrates *cyp26b1* expression in osteoblasts (arrowhead). Asterisk indicates bone matrix. (F) Model of bone matrix synthesis regulation by RA synthesis and degradation in the uninjured fin. Data are represented as mean±s.e.m. **P*<0.05, ***P*<0.01, ****P*<0.001. Scale bars: 10 µm in C; 20 µm in E. h, hours; hs, heat shock.

RA-degrading enzymes, *cyp26a1* and cyp26*c1*, could only be detected in a few single cells scattered throughout the mesenchyme and epidermis (supplementary material Fig. S2D,E), although we cannot completely rule out expression in few osteoblasts. These findings suggest that osteoblasts in the uninjured fin counteract excessive RA through Cyp26b1 activity. We tested this idea by blocking Cyp26 activity with the R115866 compound, a selective antagonist of Cyp26 enzymes (Hernandez et al., 2007; Stoppie et al.,

Development (2015) 142, 2894-2903 doi:10.1242/dev.120204

2000), and examined expression levels of *osc*, *osn*, *col1a1a* and *col10a1*. Expression was upregulated 12 h after IP injection (Fig. 1D). We conclude that Aldh1a2 in fibroblasts and Cyp26b1 in osteoblasts cooperate to control RA levels, and thus osteoblast activity in the adult fin (Fig. 1F).

### Stump osteoblasts upregulate *cyp26b1* prior to dedifferentiation

Fin amputation has previously been shown to induce upregulation of *aldh1a2* in the stump mesenchyme in proximity to the wound site, and the resulting increase in RA levels is indispensable for blastema formation (Blum and Begemann, 2012) (Fig. 2A). Of note, analyses of stump tissue at 24 hours post amputation (hpa) in *aldh1a2:gfp* fish revealed that *aldh1a2* expression remains excluded from osteoblasts upon amputation (Fig. 2B). The increase in RA synthesis in stump fibroblasts should enhance matrix synthesis in adjacent osteoblasts. However, expression of *osc* (Knopf et al., 2011; Sousa et al., 2011), *osn*, *col1a1a* and *col10a1* (supplementary material Fig. S3A) decreases upon amputation, suggesting that enhancing RA levels in osteoblasts upon fin amputation are counterproductive for their dedifferentiation. We therefore hypothesized that stump osteoblasts have to counteract rising intracellular RA levels in order to switch to a preosteoblastic state. Indeed, we detected increased expression of *cyp26b1* at 5 hpa, followed by further upregulation during the next hours (Fig. 2A). Expression levels of *cyp26a1* and *cyp26c1* were unchanged or downregulated (supplementary material Fig. S3B). We noticed that whole-mount ISH (WISH) is not sensitive enough to detect *cyp26b1* expression in the uninjured fin, but allows visualization of enhanced *cyp26b1* expression in the fin stump. Upregulated expression of *cyp26b1* could be detected in single osteoblasts within one segment length proximal to the amputation plane (Fig. 2C) as early as 12 hpa.

RA signaling employs a number of autoregulatory feedback mechanisms in order to obtain appropriate RA levels. For instance, enhanced RA levels usually cause upregulation of *cyp26* expression (Dobbs-McAuliffe et al., 2004; Hu et al., 2008; Lee et al., 2012). Accordingly, we detected increased *cyp26b1* levels in uninjured fins 10 h after RA injection and decreased levels within 12 h after a single heat shock in *hsp70I:cyp26a1* fish (supplementary material Fig. S3C). We therefore examined whether upregulation of *cyp26b1* expression in stump osteoblasts also occurs when endogenous RA is removed. Interestingly, *cyp26b1* expression was upregulated at 24 hpa despite heat shock-induced *cyp26a1* expression in *hsp70I:cyp26a1* fish (supplementary material Fig. S3D), suggesting that an RA-independent regeneration-specific program underlies upregulation of *cyp26b1*.

### Osteoblast dedifferentiation requires inactivation of RA by Cyp26b1

Osteoblast dedifferentiation is accompanied by downregulation of *osc* and upregulation of *runx2b*, a marker of immature osteoblasts (Knopf et al., 2011; Sousa et al., 2011). We found a similar upregulation of *runx2a* (not shown). In order to determine the requirement of Cyp26b1 activity for osteoblast dedifferentiation we injected fish with either R115866 or RA and examined *runx2* and *osc* expression at 10 or 24 hpa, respectively. Treatments were started 10 h before amputation (first IP at −10 hpa) to ensure sufficient drug concentrations in fin osteoblasts at the onset of dedifferentiation. Expression of *runx2b* was lower and *osc* expression was higher in RA- and R115866-treated fish than in control fish (Fig. 3A). In addition, *runx2a* expression was lower in RA-treated fish (Fig. 3A). Conversely, inhibition of RA signaling in *hsp70I:cyp26a1* fish caused enhanced *runx2* and decreased *osc* levels (Fig. 3A). These data reveal that stump osteoblasts fail to adopt characteristics of an immature state if RA levels are too high. Upregulation of *fgf20a* and *igf2b*, two positive regulators of blastema formation and proliferation (Chablais and Jazwinska, 2010; Whitehead et al., 2005), was enhanced in RA-treated fish at 10 hpa (first IP at −10 hpa) (supplementary material Fig. S4A), indicating that our treatment regime did not generally impair initiation of fin regeneration. Furthermore, in treatments starting with the first injection at 0 hpa or later, *runx2* upregulation and *osc* downregulation were largely unaffected (not shown), showing that Cyp26b1 activity is required very early in the stump. We next tested whether stump osteoblasts are able to enter the cell cycle in the absence of Cyp26b1 activity or during exogenously enhanced RA levels by assaying for 5-ethynyl-2′-deoxyuridine (EdU) incorporation at 24 hpa. The number of $EdU^{+}/ZNS\text{-}5^{+}$ cells was strongly reduced in R115866- and RA-injected fish (first IP at −10 hpa) (Fig. 3B,C). We only rarely detected dying osteoblasts in control, RA- and R115866-treated fish (data not shown), demonstrating that the decrease in proliferating osteoblasts was not due to enhanced cell death. Thus, stump osteoblasts do not start to proliferate if RA inactivation fails. An alternative explanation might be that RA signaling interferes more directly with osteoblast proliferation. However, injection of RA at 22 hpa, after many osteoblasts probably had already dedifferentiated, did not result in reduced osteoblast proliferation at 30 hpa (supplementary material Fig. S4B).

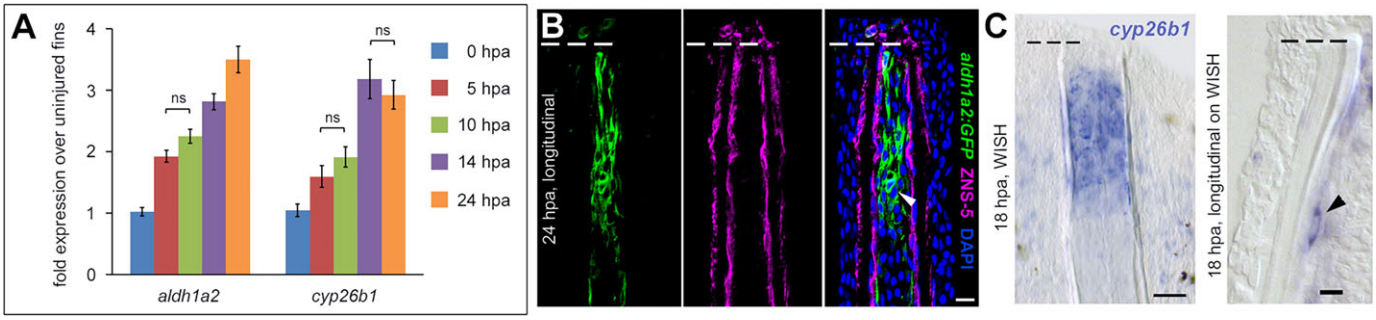


**Fig. 2. Stump osteoblasts upregulate *cyp26b1* expression.** (A) Fin amputation induces upregulation of *aldh1a2* and *cyp26b1* expression. qPCR analysis. $P<0.05$ unless noted otherwise. (B) IHC for ZNS-5 and GFP in *aldh1a2:gfp* fish at 24 hpa reveals *aldh1a2* expression in fibroblasts (arrowhead). (C) WISH indicates upregulated *cyp26b1* expression within one segment length proximal to the amputation plane at 18 hpa. Longitudinal section on WISH shows upregulated *cyp26b1* expression in single osteoblasts (arrowhead). Scale bars: 20 µm in B and C (section); 50 µm in C WISH. Dashed lines indicate amputation planes.

Development (2015) 142, 2894-2903 doi:10.1242/dev.120204

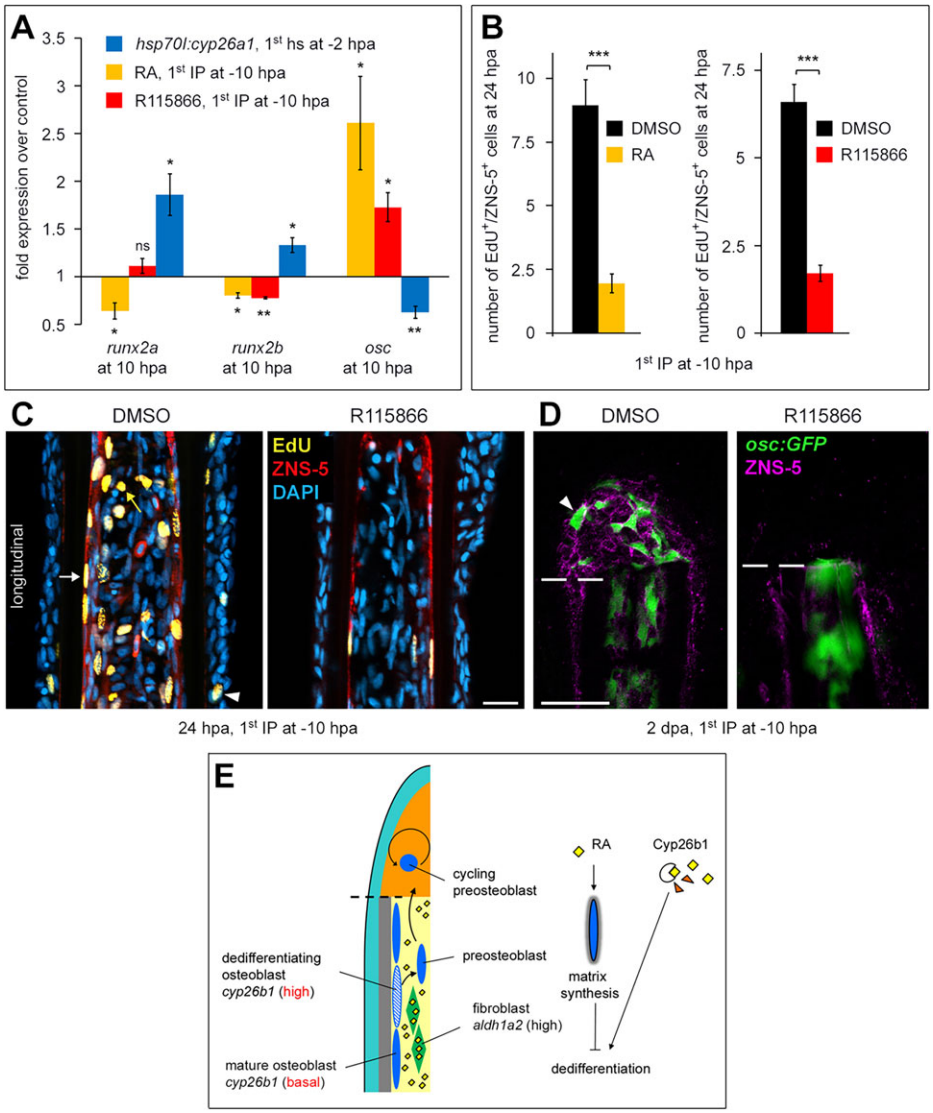


**Fig. 3. Osteoblast dedifferentiation requires RA inactivation by Cyp26b1.** RA and R115866 injections starting at −10 hpa block osteoblast dedifferentiation. Inhibition of RA signaling in *hsp70l:cyp26a1* fish positively affects dedifferentiation. (A) qPCR analysis of osteoblast markers at 10 and/or 24 hpa. (B) EdU$^+$/ZNS-5$^+$ cells per section at 24 hpa. (C) IHC for ZNS-5 combined with EdU labeling. Images show the stump region adjacent to the amputation plane. White arrow indicates EdU$^+$/ZNS-5$^+$ cell, yellow arrow denotes EdU$^+$ fibroblast, arrowhead indicates EdU$^+$ epidermal cell. (D) IHC for ZNS-5 and GFP in *osc:gfp* fish demonstrates absence of preosteoblasts in the blastema of R115866-treated fish at 2 dpa. Arrowhead indicates GFP$^+$ preosteoblast in control fish. (E) Model for Cyp26b1 function in osteoblast dedifferentiation. Data are represented as mean±s.e.m. **P*<0.05, ***P*<0.01, ****P*<0.001. ns, not significant. Scale bars: 20 µm in C; 100 µm in D. Dashed lines indicate amputation planes. hs, heat shock.

Among the three cyp26 genes, only *cyp26b1* is significantly expressed in the fin and becomes upregulated in response to fin amputation, implying that R115866 mainly acts in stump osteoblasts. Interestingly, in both RA- and R115866-treated fish (first IP at −10 hpa), regenerate length was slightly shorter at 2 dpa (supplementary material Fig. S4C,D), and the number of proliferating fibroblasts and epidermal cells was reduced at 24 hpa (supplementary material Fig. S4E). Cell death was not enhanced in fibroblasts at 24 hpa, and was only weakly enhanced in the epidermis of R115866-treated fish but not in RA-treated fish (supplementary material Fig. S4F). Notably, exogenous RA increases, rather than inhibits, fibroblast proliferation at 30 hpa, when RA treatment starts after osteoblasts have dedifferentiated (first IP at 22 hpa) (supplementary material Fig. S4G).

Dedifferentiating osteoblasts downregulate the mature osteoblast marker *osc*, and redifferentiated osteoblasts upregulate its expression between 5 and 6 dpa (Knopf et al., 2011). Owing to the persistence of GFP protein, the transgenic *osc:gfp* line can therefore be used to detect dedifferentiated osteoblasts in the early blastema (Knopf et al., 2011; Sousa et al., 2011). We assayed for the presence of GFP$^+$ preosteoblasts in the blastema of RA- and R115866-injected *osc:gfp* fish (first IP at −10 hpa). Whereas a population of GFP$^+$ cells had accumulated in the blastemas of control fish at 2 dpa, the majority of blastemas in RA- and R115866-treated fish were largely devoid (<6 cells) of GFP$^+$ cells (Fig. 3D; data not shown). Notably, RA or R115866 treatment does not interfere with preosteoblast migration (Blum and Begemann, 2015), strongly suggesting that the absence of preosteoblasts in the blastema of RA- or R115866-treated fish is due to dedifferentiation failure. Together, our data reveal that RA signaling inhibits the switch from mature osteoblasts to proliferating preosteoblasts and demonstrate that Cyp26b1 activity is crucially required for osteoblast dedifferentiation (Fig. 3E). By contrast, subsequent proliferation does not require RA inactivation. Of note, the early blastema of RA- and R115866-treated fish (first IP at −10 hpa) did not harbor ZNS-5$^+$ cells (Fig. 3D; data not shown), showing that missing dedifferentiated osteoblast were not replaced by cells that had differentiated *de novo* to osteoblasts.

### RA signaling positively controls preosteoblast proliferation

Preosteoblasts and other stump cells migrate towards the wound site, where they form a blastema within the first two days after amputation. Subsequently, a high proliferation rate in the distal blastema cells ensures regenerative outgrowth, whereas more proximal cells differentiate to rebuild the lost fin structures. Preosteoblasts form a subpopulation at proximal lateral blastema positions (Knopf et al., 2011; Sousa et al., 2011). *aldh1a2* is not

Development (2015) 142, 2894-2903 doi:10.1242/dev.120204

expressed in preosteoblasts and redifferentiated osteoblasts, but in adjacent fibroblast-derived blastema cells at 3 dpa (Fig. 4A,B). Intriguingly, although *cyp26b1* becomes upregulated in fibroblast-derived cells in the proximal medial blastema, we could not detect *cyp26b1* expression in osteoblasts at 2 or 3 dpa (Fig. 4C; data not shown). This finding indicates that, in contrast to dedifferentiating osteoblasts, preosteoblasts have ceased to remove RA. Having shown previously that RA signaling positively regulates blastema proliferation (Blum and Begemann, 2012), we next examined whether preosteoblasts also proliferate in an RA-dependent manner. As complete inhibition of RA signaling causes death of blastema cells (Blum and Begemann, 2012), we chose a mild inhibition of RA signaling, as achieved by heat-shocking *hsp70I:cyp26a1* fish at 37°C instead of 38°C, to investigate the effect of decreased RA levels on osteoblast proliferation during regenerative outgrowth. To estimate the reduction in RA levels upon heat-shocking fish at 37°C in comparison to heat-shocking at 38°C, we examined expression levels of *axin2* and *cyp26b1* at 3 dpa. Wnt/β-catenin signaling in the regenerating fin is positively regulated by RA signaling, and, accordingly, *axin2* expression becomes rapidly downregulated upon heat shock treatment in *hsp70I:cyp26a1* fish (Blum and Begemann, 2012). Similar to the uninjured fin, *cyp26b1* is a sensitive RA target during regenerative outgrowth (N.B. and G.B., unpublished). Downregulation of both genes was diminished and took longer in fish that received a 37°C heat shock at 3 dpa in comparison to fish that received a 38°C heat shock (supplementary material Fig. S5A). The number of EdU$^+$/ZNS-5$^+$ cells was strongly reduced in *hsp70I:cyp26a1* fish 3 h after a single 37°C heat shock at 3 dpa (Fig. 3D). Cell death was neither enhanced in osteoblasts nor in other cell types (data not shown). We next tested whether RA signaling is already required for preosteoblast proliferation in the stump. In contrast to blastema cells, stump cells survive well upon RA depletion (Blum and Begemann, 2012). We therefore examined the number of EdU$^+$/ZNS-5$^+$ stump cells at 30 hpa upon a 38°C heat shock at 24 hpa in *hsp70I:cyp26a1* fish. We found a strong reduction in proliferating stump cells in *hsp70I:cyp26a1 fish* (supplementary material Fig. S5B). Injection of RA at 3 dpa caused a strong increase in the number of EdU$^+$/ZNS-5$^+$ cells within 6 h after injection (Fig. 4D,E). As mentioned before, elevated RA levels between 22 and 30 hpa did not affect proliferation of stump osteoblasts (supplementary material Fig. S4B). However, this could be explained by the opposing effects of RA on dedifferentiation and proliferation. Taken together, our data demonstrate that the proliferation of preosteoblasts is positively controlled by RA.

### RA signaling prevents preosteoblast redifferentiation

After several rounds of proliferation, preosteoblasts become slow-cycling, differentiating cells in more proximal parts of the regenerate and eventually mature to matrix-producing osteoblasts (Stewart et al., 2014). The expression patterns of *aldh1a2* and *cyp26b1* at 3 dpa imply that RA concentrations within the regenerate decrease from distally high to proximally low levels (Fig. 5A and Fig. 4B,C). *aldh1a2* expression is high in fibroblast-derived cells in the distal blastema, but rapidly decreases in more proximal cells. By contrast, *cyp26b1* expression in fibroblast-derived blastema cells extends far proximally, but is absent in more distal cells, indicating that proximal fibroblast-derived blastema cells probably act as a sink for extracellular RA. Hence, osteoblasts experience different RA concentrations along the proximodistal axis. Given the positive role of RA in preosteoblast proliferation, we speculated that RA might keep preosteoblasts in a proliferative state and prevent differentiation towards the distal tip. This notion is also supported by the negative effect of RA signaling on early osteoblastogenesis during zebrafish larval development (Li et al., 2010). To test this hypothesis, we examined preosteoblast differentiation upon RA injection (first IP at 3 dpa). Because preosteoblast differentiation is accompanied by upregulation of *osx*, we used *gfp* expression in *osx:gfp* fish (*Olsp7:nlsgfp*; Spoorendonk et al., 2008) as a readout. The *osx*-free distal domain was expanded proximally in

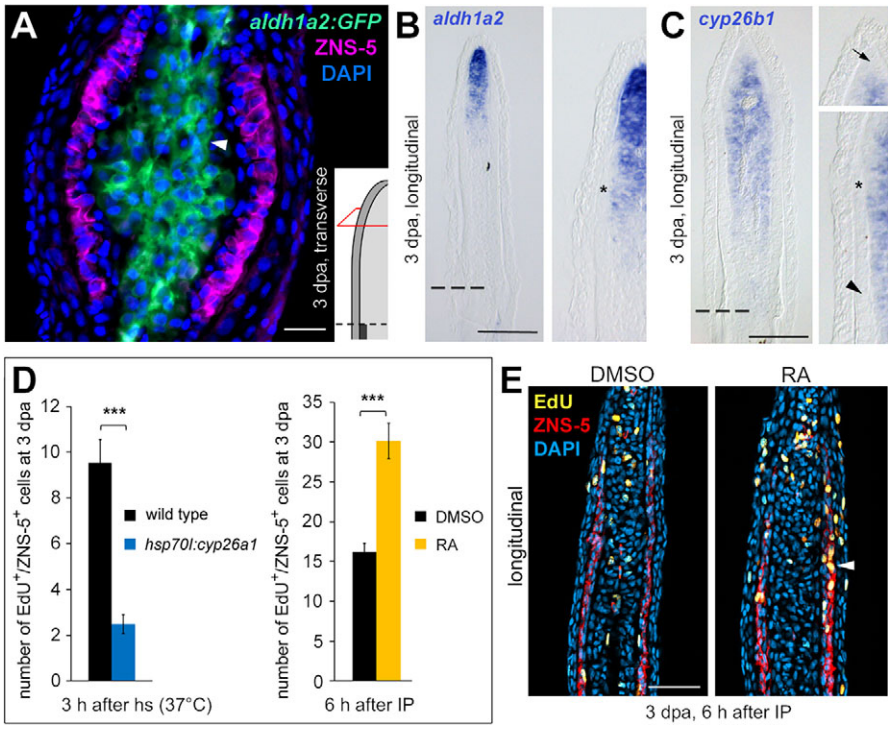


**Fig. 4. RA signaling promotes osteoblast proliferation.** (A) IHC for ZNS-5 and GFP in *aldh1a2:gfp* fish at 3 dpa reveals *aldh1a2* expression in fibroblast-derived blastema cells (arrowhead). (B) ISH for *aldh1a2* at 3 dpa shows that expression is strongest in fibroblast-derived cells in the distal blastema but weak expression reaches far proximally. Asterisk indicates distal leading edge of preosteoblasts. (C) ISH for *cyp26b1* at 3 dpa demonstrates expression in fibroblast-derived cells of the proximal medial blastema. Note absence of expression in the distal blastema (arrow) and in osteoblasts. Asterisk indicates distal leading edge of preosteoblasts, arrowhead denotes redifferentiated osteoblasts. (D,E) Inhibition of RA signaling in *hsp70I:cyp26a1* fish at 3 dpa downregulates osteoblast proliferation. RA injection causes an increase in osteoblast proliferation at 6 h after IP. (D) EdU$^+$/ZNS-5$^+$ cells per section at 3 dpa. (E) IHC for ZNS-5 combined with EdU labeling. Arrowhead indicates EdU$^+$/ZNS-5$^+$ cell. Data are represented as mean± s.e.m. ***$P$<0.001. Dashed lines indicate amputation planes. Scale bars: 20 µm in A; 100 µm in B,C,E. h, hours; hs, heat shock.

Development (2015) 142, 2894-2903 doi:10.1242/dev.120204

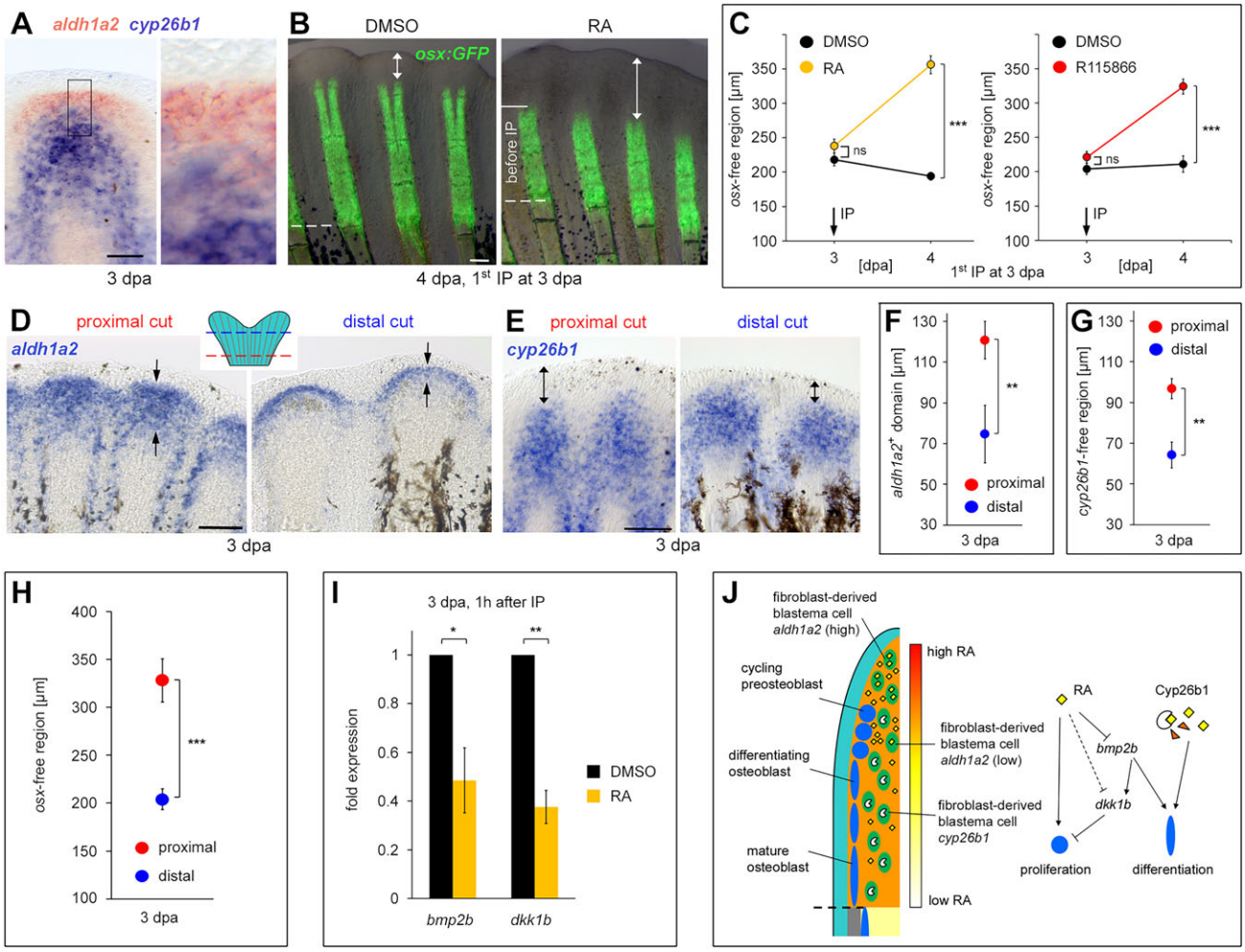


**Fig. 5. RA signaling keeps preosteoblasts in an undifferentiated state.** (A) Distal blastema cells express *aldh1a2* but not *cyp26b1*. Double WISH at 3 dpa. (B,C) RA and R115866 injections at 3 dpa block preosteoblast differentiation. (B) Live images of *osx:gfp* fish at 4 dpa demonstrate an expanded distal *osx*-free region (doubled-headed arrow) one day after RA injection. (C) Length of the *osx*-free domain. (D-H) *aldh1a2* expression (D,F), the distal *cyp26b1*-free domain (E,G) and the *osx*-free domain (H) extend further proximally in regenerates that had been amputated at a more proximal level. (D) WISH for *aldh1a2* at 3 dpa. Arrows indicate expression boundaries. (E) WISH for *cyp26b1*. Double-headed arrows indicate length of the *cyp26b1*-free region. (F-H) Length of the expression domain or of the distal expression-free region. (I) Injection of RA at 3 dpa downregulates *bmp2b* and *dkk1b* expression (qPCR analysis). (J) Model for regulation of preosteoblast differentiation by RA signaling. Data are represented as mean±s.e.m. **P*<0.05, ***P*<0.01, ****P*<0.001. Dashed lines indicate amputation planes. Scale bars: 100 µm. h, hours.

RA-treated fins 6 h after injection at 3 dpa (data not shown) and more pronounced 24 h after injection (Fig. 5B,C), indicating that preosteoblast differentiation was blocked. Expression of *cyp26b1* in proximal fibroblast-derived blastema cells suggests that RA degradation is important to lower RA levels in proximal regions, which, in turn, should allow preosteoblast differentiation. In fact, differentiation was inhibited at 4 dpa in R115866-injected fish (IP at 3 dpa) (Fig. 5C). We therefore propose that, as soon as RA levels fall below a certain threshold in more proximal parts, preosteoblasts reduce their proliferation rate and differentiate. Thus, changes in RA levels along the proximodistal blastema axis should result in a shift of the distal limit of differentiating preosteoblasts. To test this model, we took advantage of the finding that *aldh1a2* expression is expanded proximally, and that the distal limit of *cyp26b1* expression is shifted proximally in fins that have been amputated at a more proximal position (=proximal cut), relative to the situation in fins that have been amputated at a more distal position (=distal cut) (Fig. 5D-G). In such regenerates, preosteoblast differentiation would be expected to be shifted proximally due to enhanced RA synthesis and delayed RA degradation. In agreement with this view, the *osx*-free distal domain extended further proximally (Fig. 5H).

We next examined possible mechanisms that could explain how RA signaling interferes with preosteoblast differentiation. Wnt/β-catenin and BMP signaling have been shown to coordinate preosteoblast proliferation and differentiation (Stewart et al., 2014). Wnt/β-catenin signaling promotes proliferation towards the distal tip of the regenerate, whereas BMP signaling positively regulates differentiation by activating expression of *osx* and of the *dickkopf WNT signaling pathway inhibitor 1b* (*dkk1b*). *bmp2b* is expressed in differentiating preosteoblasts and is therefore probably the ligand responsible for activation of BMP signaling during differentiation. Intriguingly, we found that RA treatment downregulates expression of *dkk1b* and *bmp2b* within one hour after IP injection at 3 dpa (Fig. 5I). These data imply that RA signaling might inhibit preosteoblast differentiation by negatively interfering with BMP and promoting Wnt/β-catenin signaling. In summary, our findings suggest a model in which preosteoblast differentiation is

Development (2015) 142, 2894-2903 doi:10.1242/dev.120204

controlled by differences in RA concentrations along the proximodistal axis (Fig. 5J). High RA levels in the distal part promote proliferation and prevent premature differentiation. Conversely, non-cell-autonomous reduction of RA levels in more proximal regions through Cyp26b1 result in differentiation. Thus, both the switch from a mature to a preosteoblastic state in the stump and, vice versa, the switch back from a preosteoblastic to a mature state during regenerative outgrowth require inactivation of RA by Cyp26b1.

### RA signaling is required for bone matrix regeneration and prevents its degradation

Redifferentiated osteoblasts start to secrete bone matrix to replace the lost bone. Given the positive effect of RA signaling on bone matrix production in the uninjured fin, we assumed a similar function during regenerative outgrowth. To test this we examined transcript levels of bone matrix genes under altered RA signaling conditions at 4 and 8 dpa. Because increased RA-levels prevent preosteoblasts from differentiating, we restricted our analyses to GFP$^+$ proximal tissue in *osx:gfp* (or *osx:gfp*, *hsp70I:cyp26a1* double transgenic) fish and excluded the GFP-free distal tissue to ensure similar numbers of differentiated osteoblasts. Similar to the uninjured fin, expression of bone matrix genes was strongly downregulated after a single heat shock in *hsp70I:cyp26a1* fish at 4 (0 h after heat shock) or 8 dpa (6 h after heat shock) (Fig. 6A; supplementary material Fig. S6). By contrast, expression of bone matrix genes was largely unaffected after RA injection (Fig. 6A; supplementary material Fig. S6). Very similar results were obtained by restricting our analyses to GFP$^+$ proximal tissue in *osc:gfp* (or *osc:GFP*, *hsp70I:cyp26a1* double-transgenic) fish to ensure similar numbers of mature osteoblasts at 8 dpa (data not shown). As fin regeneration requires rapid formation of hemirays to support the new fin tissue, these results suggest that bone matrix genes are expressed at very high levels during regenerative outgrowth and cannot be

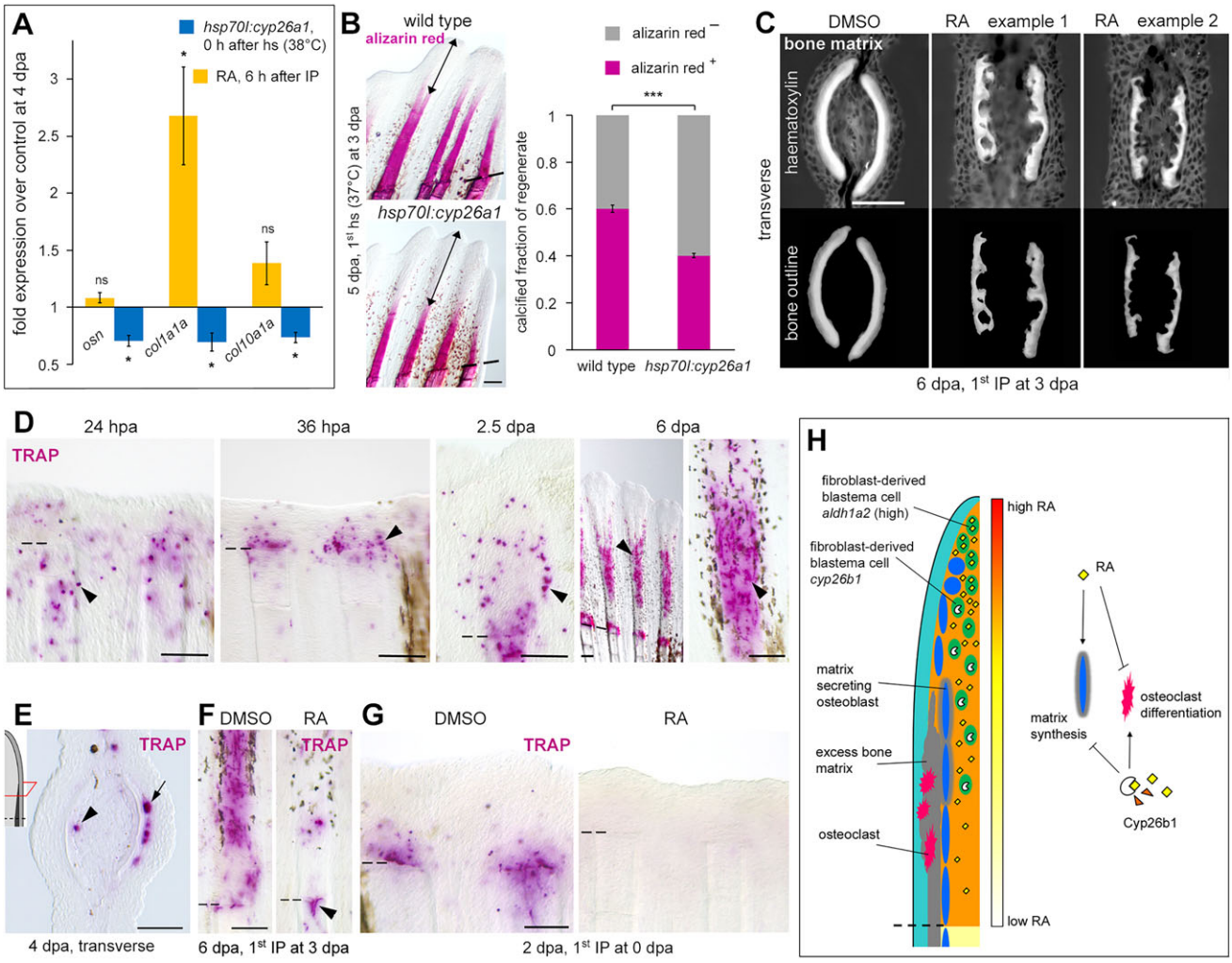


**Fig. 6. RA signaling promotes bone matrix synthesis while inhibiting degradation.** (A) qPCR analysis. Inhibition of RA signaling in *hsp70I:cyp26a1* fish at 4 dpa causes downregulation of bone matrix genes. Conversely, RA injections barely affect expression. (B) Downregulation of RA signaling in *hsp70I:cyp26a1* fish between 3 and 5 dpa results in an enlarged noncalcified (Alizarin Red$^-$) distal region (double-headed arrow) at 5 dpa. (C) RA injections starting at 3 dpa result in regeneration of irregularly shaped hemirays at 6 dpa. Hematoxylin staining. Lower panel shows hemiray outlines. (D,E) TRAP staining demonstrates presence of osteoclasts (arrowheads in D) at the wound site, in the early blastema and at the inner (arrowhead in E) and outer surface (arrow in E) of newly formed bone during regenerative outgrowth. (F) RA injections starting at 3 dpa result in fewer TRAP$^+$ cells in the regenerate but not at the wound site (arrowhead) at 6 dpa. (G) RA injections starting at 0 hpa result in absence of TRAP$^+$ cells at the wound site and in the early blastema. (H) Model for RA signaling function in bone matrix synthesis and degradation. Data are represented as mean±s.e.m. **P*<0.05, ****P*<0.01. ns, not significant. Dashed lines indicate amputation planes. Scale bars: 100 µm.

Development (2015) 142, 2894-2903 doi:10.1242/dev.120204

further upregulated by exogenous RA. We next examined regenerated bone matrix by Alizarin Red staining in *hsp70I:cyp26a1* fish that received a mild heat shock treatment (37°C), starting with the first heat shock at 3 dpa. As expected for mild inhibition of RA signaling, regenerative outgrowth was only slightly slowed down in *hsp70I:cyp26a1* fish at 5 dpa (data not shown). However, the calcified fraction of the regenerate was reduced in *hsp70I:cyp26a1* fish compared with wild-type fish (Fig. 6B). Thus, RA signaling inhibition during regenerative outgrowth interferes with bone calcification, which further demonstrates that bone matrix formation depends on RA signaling. Remarkably, RA and R115866 treatment for 3 days (first IP at 3 dpa) resulted in regeneration of irregular-shaped hemirays (Fig. 6C; data not shown). This phenotype was rather unexpected because enhanced RA signaling barely affects expression of bone matrix genes. Resorption of bone matrix by osteoclasts is an obligatory process during bone growth, remodeling and fracture healing in mammals (Väänänen et al., 2000). Moreover, osteoclasts have been shown to be involved in healing of fin ray fractures in Medaka (Takeyama et al., 2014). Thus far, osteoclasts have not been implicated in fin regeneration. We assayed for osteoclasts using tartrate-resistant acid phosphatase (TRAP) staining to analyze the presence of the osteoclast-specific TRAP. $TRAP^+$ cells were absent in the uninjured fin but could be detected after fin amputation at the wound site and within 1-2 segment lengths proximal to the amputation plane as early as 24 hpa (Fig. 6D). During regenerative outgrowth $TRAP^+$ cells were still present at the wound site. Additionally, many $TRAP^+$ cells were found at the inner and outer surface of new bone matrix (Fig. 6D,E). Whereas osteoclasts at the wound site are probably involved in healing of bone fractures that are occasionally induced during amputation, the presence of osteoclasts at newly regenerated rays suggest that hemiray regeneration requires the participation of osteoclasts.

RA signaling has been demonstrated to inhibit osteoclast differentiation *in vitro* (Conaway et al., 2009; Hu et al., 2010). We thus speculated that excess of bone matrix in RA- and R115866-treated fins was caused by defects in bone resorption. Indeed, the regenerate of RA- and R115866-treated fish were largely devoid of $TRAP^+$ cells at 6 dpa upon 3 days of treatment (Fig. 6F; data not shown). Lack of $TRAP^+$ cells suggests that enhanced RA levels either prevent osteoclast differentiation or induce osteoclast death. Alternatively, treatment might simply interfere with TRAP expression or activity. Interestingly, RA and R115866 treatment did not affect $TRAP^+$ cells at the wound site (arrowhead in Fig. 6F). Given that osteoclasts at the wound site were already present at 3 dpa when treatment was initiated, this result indicates that enhanced RA levels are likely to interfere with osteoclast differentiation. Consistently, $TRAP^+$ cells were absent from the wound site at 2 dpa in fish that received the first RA injection directly after fin amputation (Fig. 6G). These findings suggest that RA signaling controls formation of new bone matrix at two levels, by ensuring matrix synthesis by osteoblasts and by preventing degradation by osteoclasts (Fig. 6H).

## DISCUSSION

The fin blastema is a heterogeneous mixture of fate-restricted progenitor cells that are exposed to high levels of a variety of diffusible signaling molecules. Our work reveals that the amputation-induced burst of RA synthesis, which is indispensable for blastema formation and function (Blum and Begemann, 2012), is in conflict with the osteoblast regenerative program at two crucial stages, the switch from a mature to a preosteoblastic state and, vice versa, the switch back to a mature state. Specifically, we show that, although osteoblast proliferation and bone matrix synthesis requires RA from neighboring fibroblasts, dedifferentiating and redifferentiating osteoblasts have to avoid it. These findings provide novel insights into the molecular mechanisms that guide the regenerative program of osteoblasts during fin regeneration and shed light on the significant, but so far largely overlooked, issue of adverse regenerative crosstalk between neighboring fin tissues.

Mature osteoblasts in the uninjured fin continuously produce low amounts of bone matrix. Here, RA signaling positively regulates expression of bone matrix genes. Notably, RA levels in osteoblasts are determined by RA synthesis in fibroblasts and cell-autonomous RA degradation by Cyp26b1 (Fig. 1F). This cooperation between RA synthesis and degradation in adjacent tissues might help to ensure tightly controlled RA levels in osteoblasts.

Fin amputation results in enhanced RA synthesis in stump fibroblasts. The simultaneous upregulation of *cyp26b1* in osteoblasts counteracts increasing levels of RA and thus facilitates their dedifferentiation (Fig. 3E). In the absence of Cyp26b1 activity, stump osteoblasts fail to adopt an immature state. Interestingly, enhanced *cyp26b1* expression was only detected in a limited number of stump osteoblasts at a given time point, which might reflect either a short-term requirement and/or is an indication of potential asynchronous dedifferentiation of osteoblasts. Alternatively, only a small number of osteoblasts might dedifferentiate in order to establish the preosteoblast progenitor pool. It would be of interest in the future to test whether short-term upregulation of *cyp26b1* in single stump osteoblasts is sufficient to allow their dedifferentiation.

Our previous work has demonstrated that blastema formation and mesenchymal proliferation in the stump are positively regulated by RA signaling (Blum and Begemann, 2012). Unexpectedly, in this study, we found that both RA treatment and inhibition of Cyp26 activity slow down proliferation of fibroblasts and epidermal cells if treatment is initiated sufficiently early to block osteoblast dedifferentiation. Importantly, our treatment regime did not generally impair initiation of blastema formation, as shown by enhanced upregulation of *fgf20a* and *igf2b* expression. Moreover, RA treatment even increases the proliferation rate of fibroblasts when RA treatment starts too late to interfere with osteoblast dedifferentiation. Although RA treatment most likely enhances RA levels in all fin tissues, inhibition of Cyp26 activity is thought to primarily enhance RA levels in cells that express at least one of the three cyp26 genes. Thus, the spatial and temporal expression patterns of the three cyp26 genes in the fin stump imply that R115866 mainly acts in stump osteoblasts. Moreover, due to the rather small number of osteoblasts within the stump cell population, it is unlikely that *cyp26b1*-expressing osteoblasts act as a sink for extracellular RA and lower the concentration of RA within neighboring cells. Interestingly, ablation of osteoblasts during regenerative outgrowth dramatically slows down regeneration (Singh et al., 2012), suggesting that signals from osteoblasts promote proliferation of other blastema cells. We therefore propose that dedifferentiated osteoblasts might have a positive impact on other cell types already in the stump, and argue that reduced epidermal and fibroblast proliferation in the stump of RA- and R115866-treated fish might be due to disturbed osteoblast dedifferentiation.

Singh et al. (2012) have shown that, following ablation of osteoblasts in the uninjured fin, bone can regenerate normally, suggesting the presence of a $ZNS\text{-}5^-$ osteoblast progenitor population that have yet to be identified, or that other cell types can

Development (2015) 142, 2894-2903 doi:10.1242/dev.120204

transdifferentiate into osteoblasts. Although this alternative mechanism probably does not play a role in normal fin regeneration, it has been debated whether impaired osteoblast dedifferentiation can be compensated by activation of an alternative bone regeneration program. The absence of ZNS-5$^+$ cells in the blastema of RA- and R115866-treated fish indicates that missing preosteoblasts were not replaced. This finding shows that a putative alternative mechanism either does not become activated in the presence of stump osteoblasts or also requires protection from RA signaling. In contrast to dedifferentiating osteoblasts, cycling preosteoblasts do not express *cyp26b1* and require RA signaling to proliferate, suggesting that dedifferentiation and subsequent proliferation are regulated by distinct signaling mechanisms. In agreement with this notion, Fgf signaling is required for preosteoblast proliferation, but not for dedifferentiation (Knopf et al., 2011). Because *aldh1a2* expression is high in stump fibroblasts, downregulation of *cyp26b1* should allow a rapid increase in RA levels in preosteoblasts and thus might be sufficient to ensure preosteoblast proliferation upon dedifferentiation. The transition back to a differentiated state during regenerative outgrowth is prevented and proliferation is promoted by high RA levels towards the distal tip of the blastema. Moreover, the rapid downregulation of *bmp2* and *dkk1b* expression in RA-treated fish suggests that RA signaling controls preosteoblast differentiation through repression of Bmp signaling and promotion of Wnt/β-catenin signaling (Fig. 5J). Of note, differences in RA concentration along the proximodistal axis are established by opposing patterns of *aldh1a2* and *cyp26b1* expression in fibroblast-derived blastema cells. In contrast to the cell-autonomous function of Cyp26b1 in dedifferentiating stump osteoblasts, Cyp26b1 in proximal fibroblast-derived blastema cells acts non-cell-autonomously and thereby lowers extracellular RA that may diffuse into neighboring osteoblasts. Osteoblasts themselves neither produce RA nor inactivate it, indicating that RA levels in osteoblasts are determined by neighboring cells. In this model, inactivation of RA has a crucial function in controlling the proliferation rate and the position along the proximodistal axis where preosteoblasts differentiate. *shha*, a member of the Hedgehog (Hh) family, is expressed in the basal epidermal layer adjacent to preosteoblasts and has been proposed to induce their differentiation (Laforest et al., 1998). Moreover, *shha* expression was reported to become downregulated upon immersion of fish in RA (Laforest et al., 1998), suggesting that the inhibitory effect of RA on preosteoblast differentiation might be at least partly due to interfering with Hh signaling. However, we found that, although expression of *shha* requires an RA-free epidermal niche established by Cyp26a1, inhibition of Hh signaling does not interfere with preosteoblast differentiation but rather blocks proliferation (Blum and Begemann, 2015).

During regenerative outgrowth RA from fibroblast-derived blastema cells is indispensable for the expression of bone matrix genes. However, redifferentiated osteoblasts start to produce bone matrix at a position along the proximodistal axis where RA levels are already decreased, suggesting that low levels of RA are sufficient for matrix synthesis. New bone forms very rapidly during regenerative outgrowth. This requires a high rate of bone matrix secretion, raising the question of how the formation of thin, regularly shaped hemirays is ensured. The high number of osteoclasts in the regenerating fin and the striking bone phenotype in the absence of osteoclasts in RA- and R115866-treated fish is an indication for a thus far unnoticed important role of bone resorption in fin regeneration. We therefore propose that removal of excess matrix by osteoclasts is required to generate the final hemiray shape. The inhibitory effect of RA signaling on osteoclast development suggests that osteoclasts can only differentiate at positions along the proximodistal axis where RA levels are already low, a constituting regulatory mechanism that might serve to prevent premature bone resorption.

During bone development and repair, RA inhibits osteoblast differentiation and drives subsequent matrix synthesis (Laue et al., 2008; Li et al., 2010; Lie and Moren, 2012; Spoorendonk et al., 2008), whereas in the osteoclast lineage, RA signaling has been shown to promote proliferation of precursors and bone matrix resorption but blocks differentiation (Conaway et al., 2009, 2013; Hu et al., 2010). Our findings on the function of RA signaling in the formation of osteoblasts and osteoclasts during fin regeneration are consistent with those found for bone development and remodeling. Importantly, we demonstrate that RA signaling orchestrates osteoblast behavior throughout all stages of fin regeneration.

## MATERIALS AND METHODS

### Zebrafish husbandry and fin amputations

Zebrafish were raised under standard conditions at 27-28°C. Experiments were performed with 3- to 18-month-old fish. Size-matched siblings were used in all experiments. The following zebrafish lines were used: Konstanz wild type, *hsp70l:cyp26a1*$^{kn1}$ (Blum and Begemann, 2012), *aldh1a2:aldh1a2-gfp*$^{kn2}$ (Pittlik and Begemann, 2012), *Ola.bglap:egfp*$^{hu4008}$ (Knopf et al., 2011), *Ola.sp7:nls-gfp*$^{zf132}$ (Spoorendonk et al., 2008). *hsp70l:cyp26a1* fish were analyzed as heterozygotes; wild-type siblings served as controls. Reporter lines were analyzed as hetero- or homozygotes. Caudal fins were amputated along the dorsoventral axis, intersecting the median rays halfway for normal cuts, at ~30% ray length for proximal cuts and at ~70% ray length for distal cuts. Fish were allowed to regenerate for various lengths of time at 26-28°C. All animal experiments were approved by the state of Baden-Württemberg, Germany.

### Heat shock and drug treatment conditions

Heat shocks were performed once daily by transferring fish to 33-34°C for 30 min and subsequently to 38°C (or 37°C) for 1 h. IP injections were performed every 12 h for experiments until 2 dpa, and every 24 h during regenerative outgrowth. Approximately 20 µl RA or R115866 were injected. The following concentrations were used: 1 mM RA (*all-trans* RA, Sigma) in 1% DMSO/PBS; 0.67 mM R115866 (a gift from Janssen Pharmaceutica) in 10% DMSO/PBS. Control fish were injected with an equivalent concentration of DMSO/PBS. For IP injection, anesthetized fish were placed belly up in a slit in an agar plate, and the injection needle was inserted at a low angle with the tip pointing cranially close to the pelvic girdle. 1-ml tuberculin syringes (Omnifix, Braun) and 30-G hypodermic-needles (Sterican, Braun) were used.

### qPCR, analysis of cell proliferation and cell death, cryosectioning

Gene expression levels were analyzed by qPCR (for primers, see supplementary material Table S1), cell death by TUNEL staining and cell proliferation by EdU labeling. Cryosectioning was used to produce longitudinal and transverse fin sections. Further information concerning these methods, as well as descriptions of imaging and length measurements, immunohistochemistry, *in situ* hybridization, TRAP staining, Hematoxylin staining and Alizarin Red staining can be found in the supplementary material methods.

### Statistics

For quantified data, significance of differences was tested using Student's *t*-test. The numbers of specimens used for quantitative and nonquantitative experiments, and the number of specimens that showed the phenotype (for nonquantitative data) are given in supplementary material Tables S2 and S3.

#### Acknowledgements

We thank S. Schulte-Merker for transgenic fish lines, Janssen Pharmaceutica for the R115866 compound and A. Pfeifer, I. Zerenner-Fritsche, S. Leuschner and K.-H. Pöhner for fish care.

### Competing interests
The authors declare no competing or financial interests.

### Author contributions
N.B. conceived the study and designed, performed and analyzed the experiments. N.B. and G.B. wrote the manuscript.

### Funding
N.B. was supported by fellowships from the University of Konstanz and the Research Training Group (RTG) 1331 and by a travelling fellowship from The Company of Biologists. This work was supported by a grant from the Deutsche Forschungsgemeinschaft [BE 1902/6-1 to G.B.].

### Supplementary material
Supplementary material available online at
http://dev.biologists.org/lookup/suppl/doi:10.1242/dev.120204/-/DC1

### References
**Adams, S. L., Cohen, A. J. and Lassová, L.** (2007). Integration of signaling pathways regulating chondrocyte differentiation during endochondral bone formation. *J. Cell. Physiol.* **213**, 635-641.
**Akimenko, M.-A., Marí-Beffa, M., Becerra, J. and Géraudie, J.** (2003). Old questions, new tools, and some answers to the mystery of fin regeneration. *Dev. Dyn.* **226**, 190-201.
**Allen, S. P., Maden, M. and Price, J. S.** (2002). A role for retinoic acid in regulating the regeneration of deer antlers. *Dev. Biol.* **251**, 409-423.
**Blum, N. and Begemann, G.** (2012). Retinoic acid signaling controls the formation, proliferation and survival of the blastema during adult zebrafish fin regeneration. *Development* **139**, 107-116.
**Blum, N. and Begemann, G.** (2013). The roles of endogenous retinoid signaling in organ and appendage regeneration. *Cell. Mol. Life Sci.* **70**, 3907-3927.
**Blum, N. and Begemann, G.** (2015). Retinoic acid signaling spatially restricts osteoblasts and controls ray-interray organization during zebrafish fin regeneration. *Development* **142**, 2888-2893.
**Chablais, F. and Jazwinska, A.** (2010). IGF signaling between blastema and wound epidermis is required for fin regeneration. *Development* **137**, 871-879.
**Conaway, H. H., Persson, E., Halén, M., Granholm, S., Svensson, O., Pettersson, U., Lie, A. and Lerner, U. H.** (2009). Retinoids inhibit differentiation of hematopoetic osteoclast progenitors. *FASEB J.* **23**, 3526-3538.
**Conaway, H. H., Henning, P. and Lerner, U. H.** (2013). Vitamin A metabolism, action, and role in skeletal homeostasis. *Endocr. Rev.* **34**, 766-797.
**Dobbs-McAuliffe, B., Zhao, Q. and Linney, E.** (2004). Feedback mechanisms regulate retinoic acid production and degradation in the zebrafish embryo. *Mech. Dev.* **121**, 339-350.
**Dranse, H. J., Sampaio, A. V., Petkovich, M. and Underhill, T. M.** (2011). Genetic deletion of Cyp26b1 negatively impacts limb skeletogenesis by inhibiting chondrogenesis. *J. Cell Sci.* **124**, 2723-2734.
**Gemberling, M., Bailey, T. J., Hyde, D. R. and Poss, K. D.** (2013). The zebrafish as a model for complex tissue regeneration. *Trends Genet.* **29**, 611-620.
**Haas, H. J.** (1962). Studies on mechanisms of joint and bone formation in the skeleton rays of fish fins. *Dev. Biol.* **5**, 1-34.
**Hernandez, R. E., Putzke, A. P., Myers, J. P., Margaretha, L. and Moens, C. B.** (2007). Cyp26 enzymes generate the retinoic acid response pattern necessary for hindbrain development. *Development* **134**, 177-187.
**Hu, P., Tian, M., Bao, J., Xing, G., Gu, X., Gao, X., Linney, E. and Zhao, Q.** (2008). Retinoid regulation of the zebrafish cyp26a1 promoter. *Dev. Dyn.* **237**, 3798-3808.
**Hu, L., Lind, T., Sundqvist, A., Jacobson, A. and Melhus, H.** (2010). Retinoic acid increases proliferation of human osteoclast progenitors and inhibits RANKL-stimulated osteoclast differentiation by suppressing RANK. *PLoS ONE* **5**, e13305.
**Johnson, S. L. and Weston, J. A.** (1995). Temperature-sensitive mutations that cause stage-specific defects in zebrafish fin regeneration. *Genetics* **141**, 1583-1595.
**Knopf, F., Hammond, C., Chekuru, A., Kurth, T., Hans, S., Weber, C. W., Mahatma, G., Fisher, S., Brand, M., Schulte-Merker, S. et al.** (2011). Bone regenerates via dedifferentiation of osteoblasts in the zebrafish fin. *Dev. Cell* **20**, 713-724.
**Koyama, E., Golden, E. B., Kirsch, T., Adams, S. L., Chandraratna, R. A. S., Michaille, J.-J. and Pacifici, M.** (1999). Retinoid signaling is required for chondrocyte maturation and endochondral bone formation during limb skeletogenesis. *Dev. Biol.* **208**, 375-391.
**Laforest, L., Brown, C. W., Poleo, G., Géraudie, J., Tada, M., Ekker, M. and Akimenko, M. A.** (1998). Involvement of the sonic hedgehog, patched 1 and bmp2 genes in patterning of the zebrafish dermal fin rays. *Development* **125**, 4175-4184.
**Laue, K., Jänicke, M., Plaster, N., Sonntag, C. and Hammerschmidt, M.** (2008). Restriction of retinoic acid activity by Cyp26b1 is required for proper timing and patterning of osteogenesis during zebrafish development. *Development* **135**, 3775-3787.
**Laue, K., Pogoda, H.-M., Daniel, P. B., van Haeringen, A., Alanay, Y., von Ameln, S., Rachwalski, M., Morgan, T., Gray, M. J., Breuning, M. H. et al.** (2011). Craniosynostosis and multiple skeletal anomalies in humans and zebrafish result from a defect in the localized degradation of retinoic acid. *Am. J. Hum. Genet.* **89**, 595-606.
**Lee, L. M. Y., Leung, C.-Y., Tang, W. W. C., Choi, H.-L., Leung, Y.-C., McCaffery, P. J., Wang, C.-C., Woolf, A. S. and Shum, A. S. W.** (2012). A paradoxical teratogenic mechanism for retinoic acid. *Proc. Natl. Acad. Sci. USA* **109**, 13668-13673.
**Li, N., Kelsh, R. N., Croucher, P. and Roehl, H. H.** (2010). Regulation of neural crest cell fate by the retinoic acid and Pparg signalling pathways. *Development* **137**, 389-394.
**Lie, K. K. and Moren, M.** (2012). Retinoic acid induces two osteocalcin isoforms and inhibits markers of osteoclast activity in Atlantic cod (Gadus morhua) ex vivo cultured craniofacial tissues. *Comp. Biochem. Physiol. A Mol. Integr. Physiol.* **161**, 174-184.
**Lind, T., Sundqvist, A., Hu, L., Pejler, G., Andersson, G., Jacobson, A. and Melhus, H.** (2013). Vitamin a is a negative regulator of osteoblast mineralization. *PLoS ONE* **8**, e82388.
**Nallamshetty, S., Wang, H., Rhee, E.-J., Kiefer, F. W., Brown, J. D., Lotinun, S., Le, P., Baron, R., Rosen, C. J. and Plutzky, J.** (2013). Deficiency of retinaldehyde dehydrogenase 1 induces BMP2 and increases bone mass in vivo. *PLoS ONE* **8**, e71307.
**Pittlik, S. and Begemann, G.** (2012). New sources of retinoic acid synthesis revealed by live imaging of an Aldh1a2-GFP reporter fusion protein throughout zebrafish development. *Dev. Dyn.* **241**, 1205-1216.
**Poss, K. D., Shen, J., Nechiporuk, A., McMahon, G., Thisse, B., Thisse, C. and Keating, M. T.** (2000). Roles for Fgf signaling during zebrafish fin regeneration. *Dev. Biol.* **222**, 347-358.
**Poss, K. D., Keating, M. T. and Nechiporuk, A.** (2003). Tales of regeneration in zebrafish. *Dev. Dyn.* **226**, 202-210.
**Singh, S. P., Holdway, J. E. and Poss, K. D.** (2012). Regeneration of amputated zebrafish fin rays from de novo osteoblasts. *Dev. Cell* **22**, 879-886.
**Song, H. M., Nacamuli, R. P., Xia, W., Bari, A. S., Shi, Y.-Y., Fang, T. D. and Longaker, M. T.** (2005). High-dose retinoic acid modulates rat calvarial osteoblast biology. *J. Cell. Physiol.* **202**, 255-262.
**Sousa, S., Afonso, N., Bensimon-Brito, A., Fonseca, M., Simões, M., Leon, J., Roehl, H., Cancela, M. L. and Jacinto, A.** (2011). Differentiated skeletal cells contribute to blastema formation during zebrafish fin regeneration. *Development* **138**, 3897-3905.
**Spoorendonk, K. M., Peterson-Maduro, J., Renn, J., Trowe, T., Kranenbarg, S., Winkler, C. and Schulte-Merker, S.** (2008). Retinoic acid and Cyp26b1 are critical regulators of osteogenesis in the axial skeleton. *Development* **135**, 3765-3774.
**Stewart, S. and Stankunas, K.** (2012). Limited dedifferentiation provides replacement tissue during zebrafish fin regeneration. *Dev. Biol.* **365**, 339-349.
**Stewart, S., Gomez, A. W., Armstrong, B. E., Henner, A. and Stankunas, K.** (2014). Sequential and opposing activities of Wnt and BMP coordinate zebrafish bone regeneration. *Cell Rep.* **6**, 482-498.
**Stoick-Cooper, C. L., Weidinger, G., Riehle, K. J., Hubbert, C., Major, M. B., Fausto, N. and Moon, R. T.** (2007). Distinct Wnt signaling pathways have opposing roles in appendage regeneration. *Development* **134**, 479-489.
**Stoppie, P., Borgers, M., Borghgraef, P., Dillen, L., Goossens, J. A. N., Sanz, G., Szel, H., Hove, C. V. A. N., Nyen, G. V. A. N., Nobels, G. et al.** (2000). R115866 inhibits all- trans -retinoic acid metabolism and exerts retinoidal effects in rodents. *J. Pharmacol. Exp. Ther.* **293**, 304-312.
**Takeyama, K., Chatani, M., Takano, Y. and Kudo, A.** (2014). *In-vivo* imaging of the fracture healing in medaka revealed two types of osteoclasts before and after the callus formation by osteoblasts. *Dev. Biol.* **394**, 292-304.
**Tanaka, E. M. and Reddien, P. W.** (2011). The cellular basis for animal regeneration. *Dev. Cell* **21**, 172-185.
**Väänänen, H. K., Zhao, H., Mulari, M. and Halleen, J. M.** (2000). The cell biology of osteoclast function. *J. Cell Sci.* **113**, 377-381.
**Wehner, D., Cizelsky, W., Vasudevaro, M. D., Ozhan, G., Haase, C., Kagermeier-Schenk, B., Röder, A., Dorsky, R. I., Moro, E., Argenton, F. et al.** (2014). Wnt/β-catenin signaling defines organizing centers that orchestrate growth and differentiation of the regenerating zebrafish caudal fin. *Cell Rep.* **6**, 467-481.
**Weston, A. D., Hoffman, L. M. and Underhill, T. M.** (2003). Revisiting the role of retinoid signaling in skeletal development. *Birth Defects Res. C Embryo Today* **69**, 156-173.
**Whitehead, G. G., Makino, S., Lien, C.-L. and Keating, M. T.** (2005). Fgf20 is essential for initiating zebrafish fin regeneration. *Science* **310**, 1957-1960.
**Williams, J. A., Kondo, N., Okabe, T., Takeshita, N., Pilchak, D. M., Koyama, E., Ochiai, T., Jensen, D., Chu, M.-L., Kane, M. A. et al.** (2009). Retinoic acid receptors are required for skeletal growth, matrix homeostasis and growth plate function in postnatal mouse. *Dev. Biol.* **328**, 315-327.

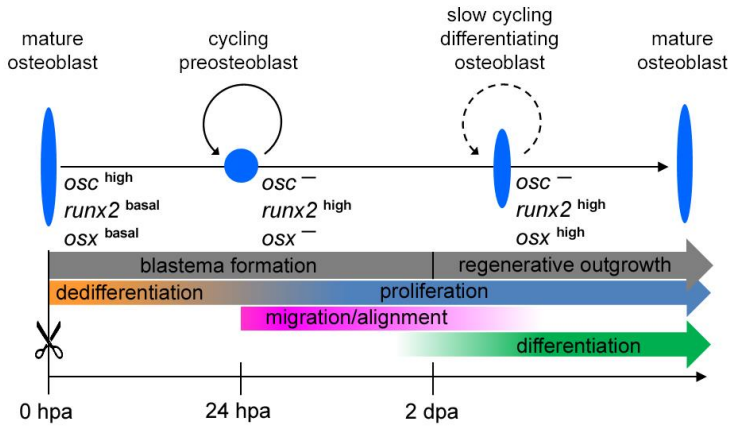


**Fig. S1. Overview of osteoblast differentiation states during fin regeneration.**

Wound epidermis formation, which overlaps with blastema formation, is not shown.

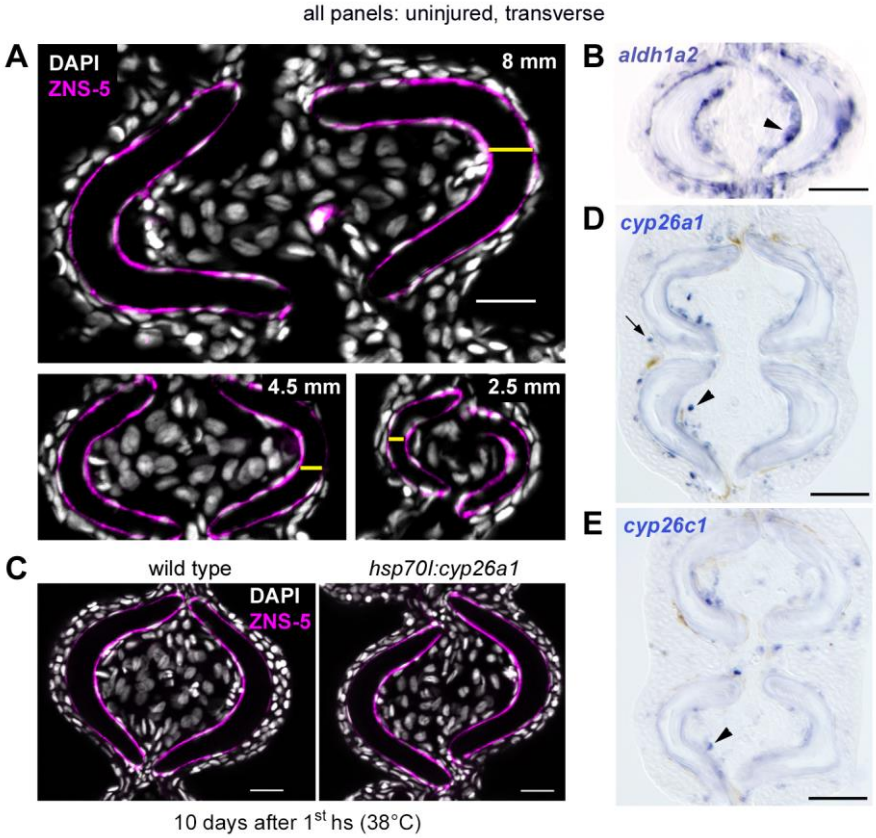


**Fig. S2. Hemiray thickness increases during fin growth; RA signaling is not required for osteoblast survival.**

(A) Sections of uninjured fins of different fin lengths reveal correlation between fin length and hemiray thickness. Fin lengths: 8, 4.5 and 2.5 mm. Yellow bars: Hemiray thickness. (B) ISH demonstrates expression of *aldh1a2* in proximity to hemirays (arrowhead). (C) Inhibition of RA signaling does not interfere with survival of mature osteoblasts. IHC for ZNS-5 demonstrates a similar number of osteoblasts in wild type and *hsp70l:cyp26a1* fish upon 10 days of heat-shock treatment. (D and E) ISH demonstrates expression of *cyp26a1* (D) and *cyp26c1* (E) in single epidermal (arrow) and mesenchymal (arrowhead) cells in uninjured fins. Scale bars: 20 µm in A, C; 50 µm in B, D and E. hs, heat-shock.

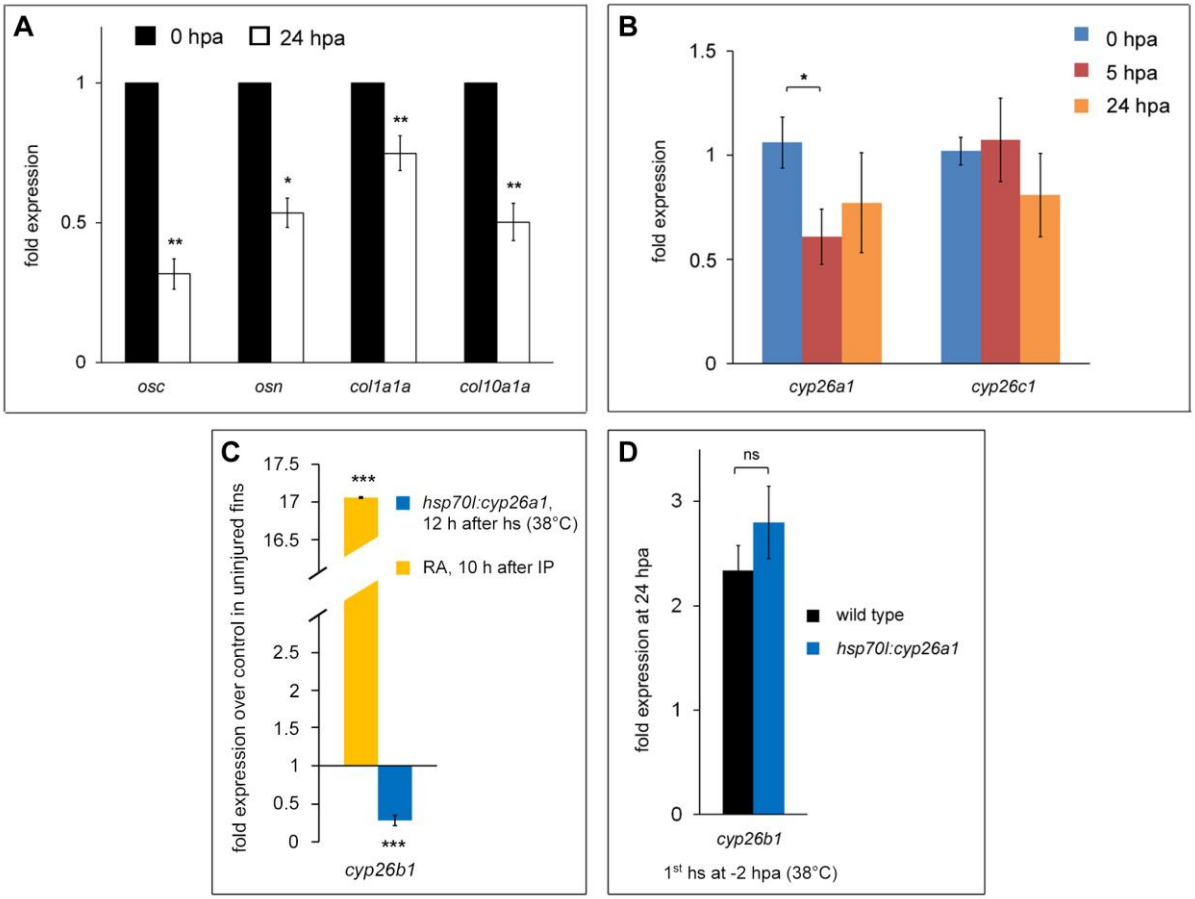


**Fig. S3. Stump osteoblasts downregulate bone matrix genes; upregulation of *cyp26b1* does not require RA signaling.**

(A) Fin amputation causes downregulation of bone matrix genes. qPCR analysis at 0 and 24 hpa. (B) Expression of *cyp26a1* and *cyp26c1* is unchanged or temporarily downregulated upon fin amputation. qPCR analysis at different time points after amputation. All not significant unless noted otherwise. (C) RA injection upregulates expression of *cyp26b1* in uninjured fins. Inhibition of RA signaling in *hsp70l:cyp26a1* fish downregulates expression. qPCR analysis. (D) Inhibition of RA signaling in *hsp70l:cyp26a1* fish does not prevent *cyp26b1* upregulation upon fin amputation. qPCR analysis at 24 hpa. Data are represented as mean±s.e.m. *p < 0.05, **p < 0.01, ***p < 0.001. ns, not significant. h, hours. hs, heat-shock.

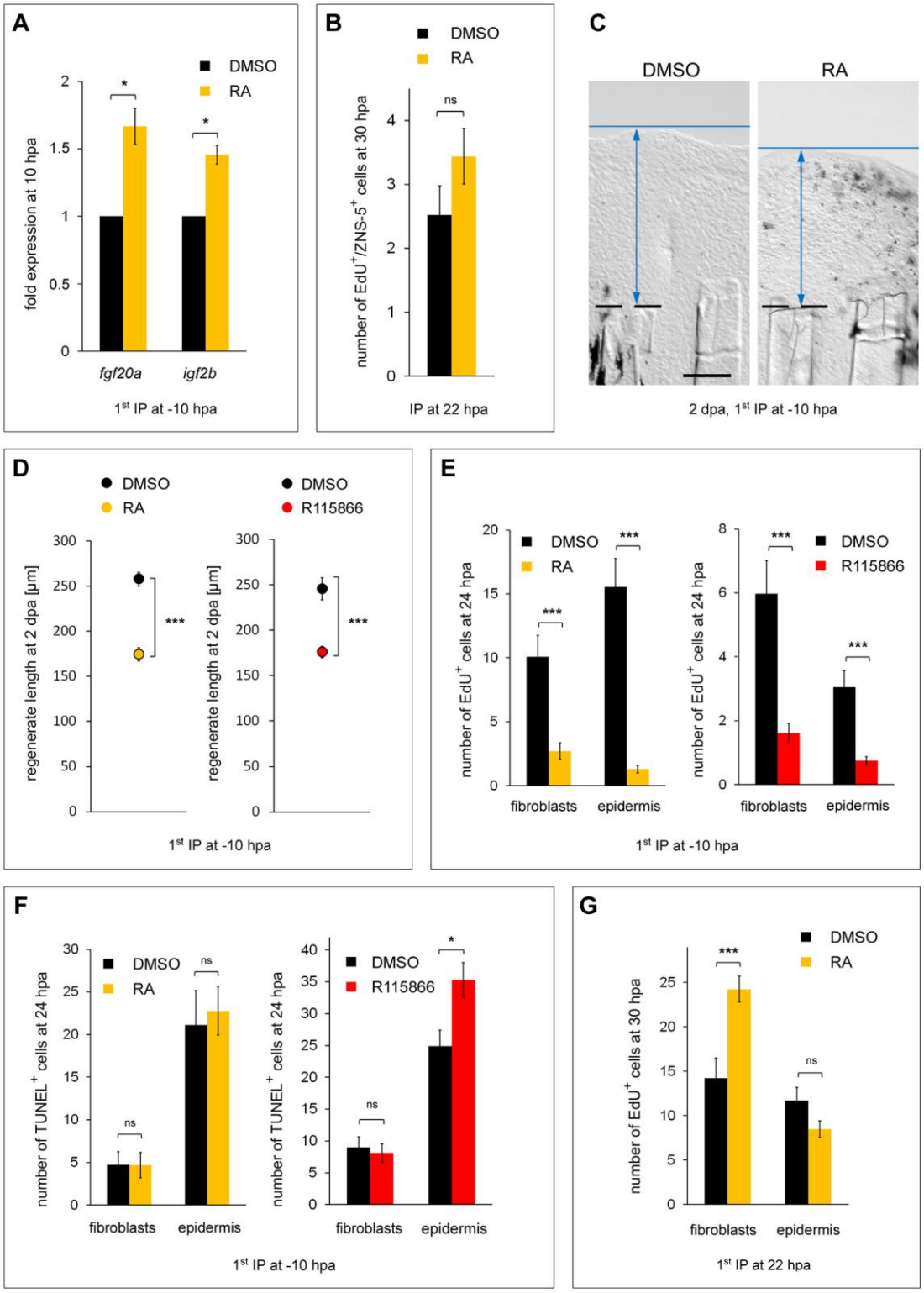


**Fig. S4. Stump osteoblasts require Cyp26b1 activity for dedifferentiation but not for subsequent proliferation**

(A) RA injections starting at -10 hpa do not prevent upregulation of *fgf20a* and *igf2b* expression in the fin stump. qPCR analysis at 10 hpa. (B) Proliferation of stump osteoblasts

is unaffected upon injection of RA at 22 hpa. $EdU^+/ZNS\text{-}5^+$ cells per section at 30 hpa. (C-F) Both RA and R115866 injections starting at -10 hpa slow down regeneration (C and D) and negatively impact proliferation of fibroblasts and epidermal cells (E), but do not increase cell death (F). (C) Fixed regenerates of RA-injected and control fish at 2 dpa. (D) Regenerate length of RA- and R115866-injected fish. (E and F) $EdU^+$ (E) or $TUNEL^+$ (F) cells per section at 24 hpa. (G) RA injection at 22 hpa promotes proliferation of fibroblasts. $EdU^+$ cells per section at 30 hpa. Data are represented as mean±s.e.m. *$p < 0.05$, ***$p < 0.001$. ns, not significant. Dashed lines indicate amputation plane.

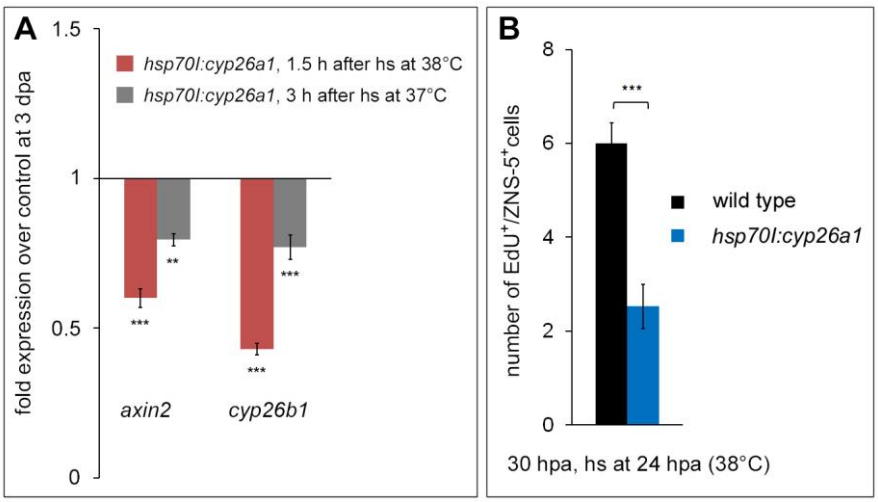


**Fig. S5. Osteoblast proliferation in the stump requires RA signaling.**

(A) Comparison of *axin2* and *cyp26b1* downregulation during regenerative outgrowth between *hsp70l:cyp26a1* fish that received a heat-shock at 37°C and *hsp70l:cyp26a1* fish that received a 38°C heat-shock. qPCR analysis at 3 dpa. (B) Inhibition of RA signaling in *hsp70l:cyp26a1* fish causes downregulation of osteoblast proliferation in the stump. $EdU^+/ZNS\text{-}5^+$ cells per section at 30 hpa. Data are represented as mean±s.e.m. **p < 0.01, ***p < 0.001. hs, heat-shock.

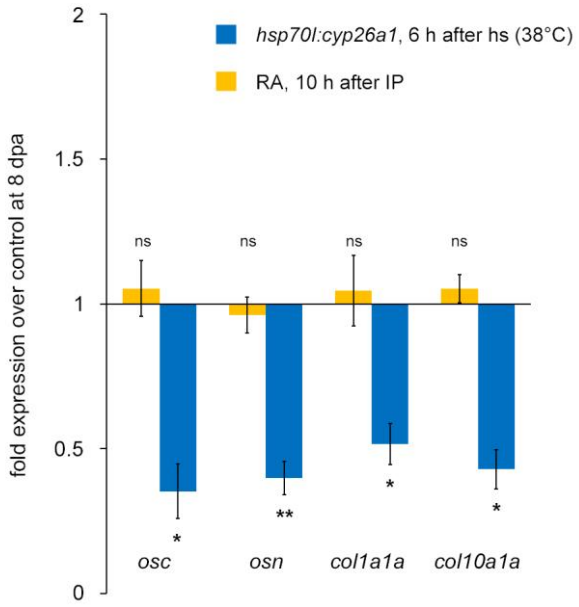


**Fig. S6. Expression of bone matrix genes at 8 dpa requires RA signaling.**

Inhibition of RA signaling in *hsp70l:cyp26a1* fish at 8 dpa causes downregulation of *osc*, *osn*, *col1a1a* and *col10a1a* expression. Conversely expression levels are unchanged in RA injected fish. qPCR analysis. Data are represented as mean±s.e.m. *p < 0.05, **p < 0.01. ns, not significant.

# Supplementary Materials and Methods

## qPCR analysis

For RNA extraction from uninjured fins, a 1 mm wide tissue stripe from the middle of the fin was harvested. For RNA extraction from 0-24 hpa, tissue within 1 mm proximal to the amputation plane was harvested. At 3, 4 and 8 dpa, tissue distal to the amputation plane was used. To analyze expression levels of bone matrix genes at 4 or 8 dpa, *osx:gfp* and *osc:gfp* (or *hsp70l:cyp26a1*, *osx:gfp* (*osc:gfp*) double transgenic) fish were used and the distal GFP-free tissue was carefully removed prior to RNA extraction by using an injection needle. Tissues from 4-10 fins were pooled for each RNA sample. Total RNA was extracted with Trizol reagent (Invitrogen) or TriPure (Roche) and treated with DNase I. Equal amounts of total RNA from each sample were reverse transcribed with SuperScript III reverse transcriptase (Invitrogen) or Maxima Reverse Transcriptase (Thermo Scientific) using anchored oligo(dT) primers. 3-4 RNA samples were reverse transcribed per Experiment (Table S2 and S3). Quantitative real-time PCR (qPCR) was performed using a C1000 thermal cycler combined with a CFX96 real-time PCR detection system (Bio-Rad) and Maxima SYBR Green qPCR Master Mix (Thermo Scientific). Primers are listed in Table S1. qPCR reactions for each cDNA pool and each target gene were performed in triplicate. qPCR data were analyzed using the CFX Manager software (Bio-Rad). *ef1a*, *tbp* and *actb1* were used as reference genes. Expression levels were normalized to expression levels of two reference genes (expression stability: Mean M <0.5) and expression ratios were calculated relative to control samples. Uninjured fins (= 0 hpa) were used as control for comparisons of expression levels between different time points. Regenerates of heat-shocked non-transgenic siblings were used as control if expression levels were examined in *hsp70l:cyp26a1* fish and regenerates of vehicle treated fish were used as control if expression levels were examined in RA- or R115866 treated fish. Reference genes were used in different combinations, depending on the treatment condition and regeneration stage. If normalization to different reference genes gave conflicting results (expression stability:

Mean M ≥0.5), results were verified by normalization to the input RNA amount by performing RiboGreen or Qubit assays (Invitrogen).

**Imaging and measurements**

Images were captured with the Zeiss AxioVision or Zeiss ZEN software on a Zeiss Stemi 2000-C stereomicroscope equipped with an AxioCam ERc5s, a Leica MZ10F stereomicroscope equipped with an AxioCam MRc or a Zeiss Axio Imager.M2 equipped with a AxioCam MRc or a AxioCam MRm. For fluorescent microscopy of IHC or EdU stained sections and whole mounts, structured illumination microscopy were used (Zeiss ApoTome.2, Zeiss Axio Imager.M2). Zeiss ZEN and Adobe Photoshop were used for image processing and length measurements. All length measurements were performed on the third dorsal and the third ventral fin ray. Measurements of hemiray thickness were performed on the third and fourth dorsal and the third and fourth ventral fin rays. Fin length was determined by measuring the length of the third ventral ray (peduncle to distal tip).

**Quantification of cell proliferation and cell death**

For quantification of cell proliferation and cell death at 24 and 30 hpa, EdU- or TUNEL-labeled epidermal cells and osteoblasts were counted within one segment length proximal to the amputation plane. Labeled stump fibroblasts were counted inside a defined area of 50 x 200 µm adjacent to the amputation plane. For quantifications at 3 dpa, labelled cells were counted in the tissue distal to the amputation plane and normalized to the regenerate length.

**Cryosectioning**

For cryosectioning, fixed fins were decalcified in 10 mM EDTA in PBT (phosphate buffered saline (PBS) containing 0.1 % Tween20) and embedded in 1.5% agar, 5% sucrose in PBS. Embedded fins were saturated in 30% sucrose in PBS and subsequently snap-frozen in Tissue-Tek O.C.T. Compound (Sakura) in liquid nitrogen. Sections were cut at 16 µm.

**Immunohistochemistry**

For IHC, fins were fixed in 4% Paraformaldehyde (PFA) in PBS for 3 hours at room temperature or over night at 4°C, transferred to MeOH and stored at –20°C. Fins were rehydrated and cryosectioned or directly subjected to whole mount IHC. Sections or fins were washed in PBT, permeabilized in PBTx (PBS containing 0.3% Triton X-100) (30 min for sections and 1 hour for whole mounts), blocked in 2% blocking reagent (Roche) in PBT and subsequently incubated with primary antibodies diluted in 2% blocking reagent over night at 4°C. After several washes in PBT, tissue was incubated with secondary antibodies diluted in PBT for 3-4 hours at room temperature or over night at 4°C. Whole mounts were transferred to 70% glycerol in PBS for imaging. Sections were counterstained with DAPI and mounted using Mowiol containing DABCO. The following antibodies and dilutions were used: mouse ZNS-5 (Zebrafish International Resource Center) 1:1500, rabbit anti-GFP (Invitrogen, A6455) 1:500. Alexa- (Invitrogen) or Atto- (Sigma) labeled secondary antibodies were used. INT/BCIP (Roche) was used to detect AP-coupled antibodies.

**TUNEL labeling**

TUNEL labeling was performed in combination with IHC for ZNS-5. Fins were fixed in 4% PFA in PBS for 3 hours at room temperature or over night at 4°C, transferred to MeOH and stored at –20°C. Fins were rehydrated and cryosectioned. Sections were washed in PBS, permeabilized for 30 min in PBTx and equilibrated in terminal deoxynucleotidyl transferase (TdT) buffer (200 mM potassium cacodylate, 25 mM Tris, 0.05% Triton X-100, 1 mM CoCl2, pH 7.2). The buffer was subsequently replaced with TdT buffer containing 0.5 µM fluorescein-12-dUTP, 40 µM dTTP and 0.02 units/µl TdT (all Thermo Scientific). Slides were incubated at 37°C for 1-2 hours and washed in PBS. Sections were blocked in 2% Blocking Reagent in PBS and incubated with anti-fluorescein-AP-coupled antibody (1:2000, Roche) and ZNS-5 antibody (1:1500) in 2% blocking reagent at 4°C over night. After several washes in PBT, TUNEL labeled cells were detected with NBT/BCIP. AP activity was subsequently quenched with 100 mM glycin (pH 2.2). Sections were washed in PBS, blocked in 2%

blocking reagent and incubated with anti-mouse-AP-coupled antibody (1:500, Sigma). ZNS-5 labeled cells were detected with INT/BCIP (Roche). Sections were mounted using Mowiol.

**EdU labeling**

For EdU labelling, fish were IP injected with approximately 20 µl of 2.5 mg/ml EdU (Jena Bioscience) in PBS 1 hour (for analyses at 24 or 30 hpa) or 30 min (for analyses at 3 dpa) prior to fixation. Fins were fixed in 4% PFA in PBS for 3 hours at room temperature or over night at 4°C, transferred to MeOH and stored at –20°C. Fins were rehydrated, washed in PBT and permeabilized in PBTx for 30 min. Subsequently, fins were equilibrated in 100 mM Tris/HCl pH 8 and EdU was detected using a copper-catalyzed azide-alkyne click chemistry reaction (0.6 µM Cy3- or Fluor488- labeled azides (Jena Bioscience), 100 mM Tris, 1 mM CuSO4, 100 mM ascorbic acid, pH 8) with 20 min incubation time. Labeled fins were cryosectioned. For EdU/IHC double staining, EdU labeling was performed on whole mounts and IHC was subsequently performed on sections.

**In situ hybridization**

Digoxigenin (DIG)- or fluorescein labeled RNA antisense probes were synthesized from cDNA templates: *aldh1a2* (Grandel et al., 2002), *cyp26a1* (Kudoh et al., 2002), *cyp26b1* (Hernandez et al., 2007), *cyp26c1* (Gu et al., 2005). WISH or ISH on sections was performed as previously described (Blum and Begemann, 2012). For double WISH DIG- and fluorescein-labeled probes were hybridized simultaneously. Fins were first incubated with anti-DIG-AP coupled antibody and color reaction was performed with BCIP/NBT. AP activity was quenched with 100 mM glycin (pH 2.2) and fluorescein was detected by using anti-fluorescein-AP coupled antibody and INT/BCIP as substrate.

**TRAP staining**

For TRAP staining, fins were fixed in 4% PFA in PBS for 3 hours at room temperature or over night at 4°C, washed in PBT and permeabilized in PBTx for 30 min. Subsequently, fins were equilibrated in TRAP Puffer (0.1M NaAcetate, 0.1M acetic acid, 50mM NaTartrate) and

color reaction was performed in TRAP buffer containing 0.1 mg/ml Naphtol AS-MX phosphate (Sigma) and 0.3 mg/ml Fast Red Violet LB (Sigma). Labeled fins were transferred to 70% glycerol in PBS for imaging or were cryosectioned.

**Hematoxylin staining**

Fins were fixed in 4% PFA in PBS, transferred to methanol and stored at –20°C. Fins were rehydrated prior to cryosectioning. Sections were stained in Mayer's Hematoxylin Solution (Sigma) for 3-5 minutes, washed in water and cleared in 0.37% HCl in 70% ethanol for 5-10 seconds.

**Alizarin Red staining**

For Alizarin Red staining, fins were fixed in 4% PFA in PBS, transferred to MeOH and stored at -20°C. Fins were rehydrated, washed in PBT and stained in 0.1% Alizarin Red in 0.5% KOH overnight. Excess dye was removed by several washes in 0.5% KOH. Stained fins were transferred to 70% glycerol in 0.5% KOH for imaging.

## Supplementary References

**Grandel, H., Lun, K., Rauch, G.-J., Rhinn, M., Piotrowski, T., Houart, C., Sordino, P., Küchler, A. M., Schulte-Merker, S., Geisler, R., et al.** (2002). Retinoic acid signalling in the zebrafish embryo is necessary during pre-segmentation stages to pattern the anterior-posterior axis of the CNS and to induce a pectoral fin bud. *Development* **129**, 2851–65.

**Gu X, Xu F, Wang X, Gao X, Z. Q.** (2005). Molecular cloning and expression of a novel CYP26 gene (cyp26d1) during zebrafish early development. *Gene Expr. Patterns* **5**, 733–739.

**Kudoh, T., Wilson, S. W. and Dawid, I. B.** (2002). Distinct roles for Fgf, Wnt and retinoic acid in posteriorizing the neural ectoderm. *Development* **129**, 4335–46.

**Table S1. Primer sequences for qPCR experiments.**

| Gene | Forward primer | Reverse primer |
|---|---|---|
| *aldh1a2* | GAGAGAGACAGTGCTTACCTTGC | CACAAAGAAGCAGGGGAGG |
| *axin2* | GCAGCACAGTTGATAGCCAG | GTCTTGGCTGGCACATATCC |
| *bactin1* | TTGCTCCTTCCACCATGAAG | CTTGCTTGCTGATCCACATC |
| *bmp2b* | CTGCTGACCACAAGTTTTCG | CAAAGACAGCAGCAATCCC |
| *col10a1a* | GCATTCTTCTTCTCCTGGTG | CCTGAACCCCAACCCCC |
| *col1a1a* | CAAAACAACGAAAACATCCC | GCATTTGGTTTCGCTCTTTC |
| *cyp26a1* | GATGGGAGCTGATAATGTG | CCTGAACCTCCTCTCTGACC |
| *cyp26b1* | GCTGGCTGCGTGTTTAGTG | GCCGTCCCAGTAGATGAGTC |
| *cyp26c1* | GCAGGAGACAAGGAGGAGG | GCTTCTGCCGTCTCGTGTG |
| *dkk1b* | ATGCCAGAGACACTAAATGAACA | TATGAAGGAAACCAGTTGAAAAA |
| *ef1a* | TACGCCTGGGTGTTGGACAAA | TCTTCTTGATGTATCCGCTGAC |
| *fgf20a* | AAAAGCTGTCAGCCGAGTGT | TGGACGTCCCATCTTTGTTG |
| *igf2b* | GCAGGTCATTCCAGTGATGC | TCTGAGCAGCCTTTCTTTGC |
| *osc* | CCTGATGACTGTGTGTCTGAG | CGCTTCACAAACACACCTTC |
| *osn* | GTGGAGGATGTTATTGCTGAG | GGGGCAGGTCAAAGGGTC |
| *runx2a* | GATTTGTGCTCCCGCTTTAG | CTGCTGGACGGCGGACTG |
| *runx2b* | GGAGTGGAGGGAGATGGAAG | TAGCGAGTGGAAGAGTACAGATTG |
| *tbp* | CGGTGGATCCTGCGAATTA | TGACAGGTTATGAAGCAAAACAACA |

**Table S2. Number of specimens used in quantitative and nonquantitative experiments (Figs. 1-6).** Numbers for corresponding experiments, which are not shown in the figure, are included. For nonquantitative experiments: the first number indicates the number of specimens showing the phenotype, the second number the total number.

| Figure | n= |
|---|---|
| 1B | 33-46 rays per position along the proximodistal axis in adult fish;<br>27-39 rays per fin length class |
| 1D | 3 cDNA samples per condition |
| 2A | 3 cDNA samples per time point |
| 3A | 3 cDNA samples per condition |
| 3B | RA: DMSO= 15 sections (4 fins), RA= 35 sections (5 fins);<br>R115866: DMSO= 35 sections (6 fins), R115866=53 sections (6 fins) |
| 3D | RA: DMSO= 36/175 rays, RA= 181/237 rays;<br>R115866: DMSO= 35/211 rays, RA= 122/223 rays |
| 4D | wild type= 24 sections (6 fins), *hsp70l:cyp26a1*= 32 sections (10 fins);<br>DMSO= 31 sections (8 fins), RA=29 sections (6 fins) |
| 5C | RA: DMSO= 12 rays, RA= 12 rays; R115866: DMSO= 12 rays, R115866= 12 rays |
| 5F | proximal= 7 rays, distal=7 rays |
| 5G | proximal= 7 rays, distal=8 rays |
| 5H | proximal= 13 rays, distal=12 rays |
| 5I | 3 cDNA samples per condition |
| 6A | 3-4 cDNA samples per condition |
| 6B | wild type= 16 rays (8 fins), *hsp70l:cyp26a1*= 16 rays (8 fins); |
| 6C | RA: DMSO= 0/5 fins , RA= 6/6 fins;<br>R115866: DMSO= 0/6 fins, R115866= 6/6 fins |
| 6F | RA: DMSO= 0/6 fins , RA= 5/6 fins;<br>R115866: DMSO= 0/5 fins, R115866= 4/5 fins |
| 6G | DMSO= 0/5 fins , RA= 6/6 fins |

**Table S3. Number of specimens used in quantitative and nonquantitative experiments (Figs. S1-4).** Numbers for corresponding experiments, which are not shown in the figure, are included. For nonquantitative experiments: the first number indicates the number of specimens showing the phenotype, the second number the total number.

| Figure | n= |
|---|---|
| S2C | wild type= 5/5 fins, *hsp70l:cyp26a1*= 5/5 fins |
| S3A | 3 cDNA samples per time point |
| S3B | 3 cDNA samples per time point |
| S3C | 3 cDNA samples per condition |
| S3D | 3 cDNA samples per condition |
| S4A | 3 cDNA samples per condition |
| S4B | DMSO= 25 sections (5 fins), RA= 25 sections (4 fins) |
| S4D | RA: DMSO= 30 rays, RA= 35 rays;<br>R115866: DMSO= 24 rays, R115866= 26 rays |
| S4E | RA: DMSO= 15 sections (4 fins), RA= 35 sections (5 fins);<br>R115866: DMSO= 35 sections (6 fins), R115866=53 sections (6 fins) |
| S4F | RA: DMSO= 16 sections (5 fins), RA= 25 sections (6 fins);<br>R115866: DMSO= 27 sections (7 fins), R115866=30 sections (7 fins) |
| S4G | DMSO= 25 sections (5 fins), RA= 25 sections (4 fins) |
| S5A | 3 cDNA samples per condition |
| S5B | wild type= 17 sections (6 fins), *hsp70l:cyp26a1*= 17 sections (6 fins) |
| S6 | 3 cDNA samples per condition |